



**Fermi National Accelerator Laboratory**

**FERMILAB-TM-2053**

# **Introduction to Collective Instabilities—Longitudinal and Transverse**

King-Yuen Ng

*Fermi National Accelerator Laboratory  
P.O. Box 500, Batavia, Illinois 60510*

October 1998

## **Disclaimer**

*This report was prepared as an account of work sponsored by an agency of the United States Government. Neither the United States Government nor any agency thereof, nor any of their employees, makes any warranty, expressed or implied, or assumes any legal liability or responsibility for the accuracy, completeness, or usefulness of any information, apparatus, product, or process disclosed, or represents that its use would not infringe privately owned rights. Reference herein to any specific commercial product, process, or service by trade name, trademark, manufacturer, or otherwise, does not necessarily constitute or imply its endorsement, recommendation, or favoring by the United States Government or any agency thereof. The views and opinions of authors expressed herein do not necessarily state or reflect those of the United States Government or any agency thereof.*

## **Distribution**

*Approved for public release; further dissemination unlimited.*

## **Copyright Notification**

*This manuscript has been authored by Universities Research Association, Inc. under contract No. DE-AC02-76CHO3000 with the U.S. Department of Energy. The United States Government and the publisher, by accepting the article for publication, acknowledges that the United States Government retains a nonexclusive, paid-up, irrevocable, worldwide license to publish or reproduce the published form of this manuscript, or allow others to do so, for United States Government Purposes.*

INTRODUCTION TO COLLECTIVE INSTABILITIES  
— LONGITUDINAL AND TRANSVERSE

King-Yuen Ng

*Fermi National Accelerator Laboratory,<sup>†</sup> P.O. Box 500, Batavia, IL 60510*

1998 OCPA Accelerator School

August 3-12, 1998

Hsinchu, Taiwan

---

<sup>†</sup>Operated by the Universities Research Association, Inc., under contract with the U.S. Department of Energy.

# CONTENTS

- 1 Wakes and impedances
    - 1.1 Wake functions
    - 1.2 Coupling impedancesExercises
  - 2 Longitudinal phase space
    - 2.1 Equations of motion
    - 2.2 Vlasov equationExercises
  - 3 Potential-well distortion  
Exercises
  - 4 Longitudinal microwave instability
    - 4.1 Dispersion relation
    - 4.2 Landau damping
    - 4.3 Self-bunching
    - 4.4 Overshoot and bunch lengthening
    - 4.5 ObservationExercises
  - 5 Longitudinal coupled-bunch instabilities
    - 5.1 Sacherer integral equation
    - 5.2 Time domain
    - 5.3 Rf-detuning and Robinson's stability criteriaExercises
  - 6 Transverse instabilities
    - 6.1 Sacherer integral equation
    - 6.2 Solution of Sacherer integral equations
    - 6.1 Sacherer sinusoidal modes of excitation
    - 6.2 Chromaticity frequency shiftExercises
  - 7 Transverse coupled-bunch instabilities
    - 7.1 Resistive wall
    - 7.2 Narrow resonancesExercises
  - 8 Head-tail instabilities  
Exercises
  - 9 Mode-mixing
    - 9.1 Transverse
    - 9.2 LongitudinalExercises
- References

# 1 WAKES AND IMPEDANCES

A positively charged test particle at rest has static electric field going out radially in all directions. In motion with velocity  $v$ , magnetic field is generated. As the particle velocity approaches  $c$ , the velocity of light, the electric and magnetic fields are pancake-like, the electric field is radial and magnetic field azimuthal (the Liénard-Wiechert fields). It is worth pointing out that no matter how far away, this pancake is always perpendicular to the path of motion. In other words, the fields move with the test particle without any lagging behind as illustrated in Fig. 1.

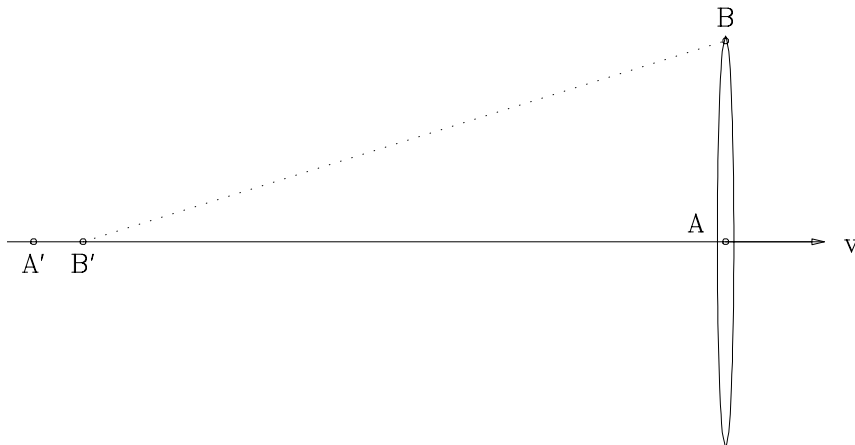


Figure 1: Schematic drawing of pan-cake electromagnetic fields emitted by an ultra-relativistic particle traveling with velocity  $v$ . The pan-cake is always perpendicular to the path of the particle and travels in pace with the particle no matter how far away the fields are from the particle. There is no violation of causality because fields at points  $A$  and  $B$  come from the particle at different locations. Fields from  $A$  are from  $A'$  at a time  $AA'/v$  ago, while fields at  $B$  from point  $B'$ , at a time  $AB'/v$  ago, where  $AA' = BB'$ .

When placed inside a perfectly conducting beam pipe, the pancake of fields is trimmed by the beam pipe. A ring of negative charges will be formed on the wall of the beam pipe where the electric field ends, and these image charges will travel at the same pace as the particle, creating the so called *image current*. If the wall of the beam pipe is not perfectly conducting or contains discontinuities, the movement of the image charges will be slowed down, thus leaving electromagnetic fields behind. For example, when coming across a cavity, the image current will flow into the wall of the cavity, creating fields trapped inside the cavity. These fields left behind by the particle are called wake fields, which are important because they will influence the motion of the particles that follow.

## 1.1 WAKE FUNCTIONS

Consider a test particle carrying charge  $q_1$  traveling with velocity  $v$  longitudinally along a designated path in a beam pipe. A witness particle of charge  $q_2$  at a distance  $z$  behind sees a longitudinal force  $F_0^{\parallel}$  and a transverse force  $F_0^{\perp}$  due to the wake fields of the test particle. In general, these forces depend also on the location  $s$  of the test particle along the beam pipe. However, when these forces are integrated over  $s$  for a

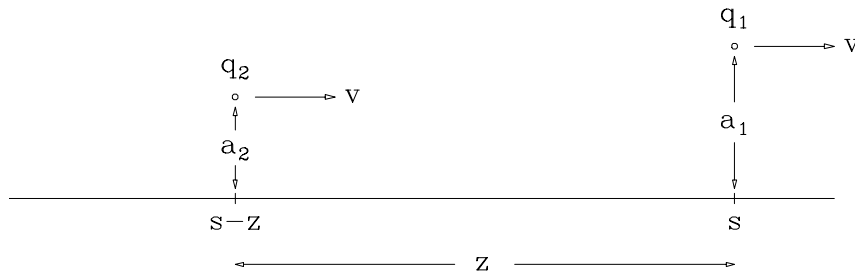


Figure 2: Test particle with charge  $q_1$  at an offset of  $a_1$  from the designated path leaves wake fields to the witness particle with charge  $q_2$  at an offset of  $a_2$  at a distance  $z$  behind.

long length  $\ell$  of the beam pipe, they become functions of  $z$  only. For a circular machine,  $\ell$  is taken as the circumference  $C$ . The *longitudinal wake function* is defined as

$$W'_0(z) = \frac{\langle F_0^{\parallel} \rangle \ell}{q_1 q_2}, \quad (1.1)$$

where  $\langle F_0^{\parallel} \rangle \ell$  denotes the longitudinal integrated wake force. As defined,  $W'_0(z)$  has the dimension of force-length per charge square or Ohms/time.

If the path of the test particle is displaced transversely by  $a_1$  from the designated path, the witness particle displaced by  $a_2$  at a distance  $z$  behind, as illustrated in Fig. 2, will see a longitudinal force  $F_1^{\parallel}$  and a transverse force  $F_1^{\perp}$ . The *transverse wake function* is defined by

$$W_1(z) = \lim_{a_1, a_2 \rightarrow 0} \frac{(\langle F_1^{\perp} \rangle - \langle F_0^{\perp} \rangle) \ell}{a_1 q_1 q_2}, \quad (1.2)$$

which has the dimension of Ohms/(time-length).

Notice that when the designated particle path is the axis of symmetry of a cylindrical beam pipe, we can expand everything into azimuthal harmonics  $m = 0, 1, 2, \dots$ . Then  $W'_0(z)$  is called the azimuthal monopole ( $m = 0$ ) longitudinal wake function. Also, the on-axis transverse force  $F_0^{\perp} = 0$ , and  $W_1(z)$  is called the azimuthal dipole ( $m = 1$ ) transverse wake function. Similar to Eq. (1.2), the longitudinal dipole wake function can be defined as

$$W'_1(z) = \lim_{a_1, a_2 \rightarrow 0} \frac{(\langle F_1^{\parallel} \rangle - \langle F_0^{\parallel} \rangle) \ell}{a_1 a_2 q_1 q_2}, \quad (1.3)$$

where  $a_2$  is the offset of the witness particle from the designated orbit.

As a result of the Panofsky-Wenzel theorem, for any azimuthal  $m \neq 0$ , the longitudinal wake function  $W'_m(z)$  is the derivative of the transverse wake function  $W_m(z)$ , which explains why a prime has been placed in the longitudinal wake in Eq. (1.1). In our discussion below, we shall concentrate on only the lowest azimuthal modes; i.e.,  $W'_0$  for the longitudinal and  $W_1$  for the transverse.

When the particle velocity  $v$  approaches the velocity of light, the wake functions have to obey the causality condition that they vanish<sup>†</sup> when  $z < 0$ . This is the situation for most electron machines and high-energy proton machines. For our discussions below, we will continue to use  $v$  instead of  $c$  in most

<sup>†</sup>Some authors prefer to define the wake function to be zero for  $z > 0$  and nonzero otherwise.

places, because we would like to derive stability conditions and growth rates also for machines that are not ultra-relativistic. However, strict causality will be imposed.

## 1.2 COUPLING IMPEDANCES

Beam particles form a current, of which the component with frequency  $\omega/(2\pi)$  is  $I_0(s, t) = \hat{I}_0 e^{-i\omega(t-s/v)}$ , where  $\hat{I}_0$  may be complex. This current component at location  $s$  and time  $t$  will be affected by the wake of the preceding beam particles that pass the point  $s$  at time  $t-z/v$  with the charge element  $I_0(s, t-z/v)dz/v$ . The total voltage seen will be

$$V(s, t) = \int_{-\infty}^{\infty} \hat{I}_0 e^{-i\omega[t-(s+z)/v]} W_0'(z) \frac{dz}{v} = I_0(s, t) \int_{-\infty}^{\infty} e^{i\omega z/v} W_0'(z) \frac{dz}{v} . \quad (1.4)$$

Thus we can identify the *longitudinal coupling impedance* of the vacuum chamber as

$$Z_0^{\parallel}(\omega) = \int_{-\infty}^{\infty} e^{i\omega z/v} W_0'(z) \frac{dz}{v} . \quad (1.5)$$

Similarly, when the current is displaced transversely by  $a_1$ , the transverse force, averaged over the ring circumference  $C$ , acting on a current particle is obtained by summing the charge element  $I_0(s, t-z/v)dz/v$  passing  $s$  at time  $t-z/v$ ,

$$\langle F_1^{\perp}(s, t) \rangle = \frac{q_2 a_1}{C} \int_{-\infty}^{\infty} \hat{I}_0 e^{-i\omega[t-(s+z)/v]} W_1(z) \frac{dz}{v} = \frac{q_2 a_1}{C} I_0(s, t) \int_{-\infty}^{\infty} e^{i\omega z/v} W_1(z) \frac{dz}{v} . \quad (1.6)$$

We identify the *transverse coupling impedance* of the vacuum chamber as

$$Z_1^{\perp}(\omega) = -\frac{i}{\beta} \int_{-\infty}^{\infty} e^{i\omega z/v} W_1(z) \frac{dz}{v} , \quad (1.7)$$

where the  $-i$  takes into account the fact that the force lags the displacement by  $\frac{1}{2}\pi$  and the Lorentz factor  $\beta = v/c$  is a convention. In both Eqs. (1.4) and (1.6), the lower limits of integration have been extended to  $-\infty$ , because the wake functions vanish when  $z < 0$ . From Eq. (1.6), it is evident that we can also compute the transverse impedance by integrating the wake force averaged over one turn according to

$$Z_1^{\perp}(\omega) = -\frac{i}{q_2 \beta I_0 a_1} \int_0^C \langle F_1^{\perp} \rangle ds , \quad (1.8)$$

where  $I_0 a_1$  represents the dipole current. Note that the longitudinal impedance is mostly the monopole ( $m = 0$ ) impedance and the transverse impedance is mostly the dipole ( $m = 1$ ) impedance, if the beam pipe cross section is close to circular and the particle path is close to the pipe axis. They have the dimensions of Ohms and Ohms/length, respectively. The impedances have the following properties:

1.  $Z_0^{\parallel}(-\omega) = [Z_0^{\parallel}(\omega)]^*$  ,  $Z_1^{\perp}(-\omega) = -[Z_1^{\perp}(\omega)]^*$  (1.9)

2.  $Z_0^{\parallel}(\omega)$  and  $Z_1^{\perp}(\omega)$  are analytic with poles only in the lower half  $\omega$ -plane. (1.10)

3.  $Z_m^{\parallel}(\omega) = \frac{\omega}{v} Z_m^{\perp}(\omega)$  , for cylindrical geometry and each azimuthal harmonic  $m \neq 0$  . (1.11)

4.  $\text{Re } Z_0^{\parallel}(\omega) \geq 0$  ,  $\text{Re } Z_1^{\perp}(\omega) \geq 0$  , when  $\omega > 0$  , (1.12)

5.  $\int_0^{\infty} d\omega \text{Im } Z_1^{\perp}(\omega) = 0$  ,  $\int_0^{\infty} d\omega \frac{\text{Im } Z_0^{\parallel}(\omega)}{\omega} = 0$  , if the beam pipe has the same entrance and exit cross section. (1.13)

The first follows because the wake functions are real, the second from the causality of the wake functions, and the third from the Panofsky-Wenzel theorem [1] between transverse and longitudinal electromagnetic forces.  $\text{Re } Z_m^\parallel(\omega) \geq 0$  is the result of the fact that the total energy of a particle or a bunch cannot be increased after passing through a section of the vacuum chamber where there is no accelerating external forces, while  $\text{Re } Z_m^\perp(\omega) \geq 0$  when  $\omega > 0$  follows from the Panofsky-Wenzel theorem. The fifth property follows from that fact that  $W_1^\perp(0) = 0$ .

For a pure resistance  $R$ , the longitudinal wake is  $W_0'(\omega) = R\delta(z/v)$ . At low frequencies, the wall of the beam pipe is inductive. This wake function is  $W_0'(\omega) = L\delta'(z/v)$ , where  $L$  is the inductance. For a nonrelativistic beam of radius  $a$  inside a circular beam pipe of radius  $b$ , the space-charge impedance is<sup>‡</sup>

$$Z_0^\parallel = i \frac{\omega}{\omega_0} \frac{Z_0}{2\gamma^2\beta} \left( \frac{1}{2} + 2 \ln \frac{b}{a} \right), \quad (1.14)$$

where  $Z_0 \approx 377 \Omega$  is the impedance of free-space,  $\omega_0/(2\pi)$  is the revolution frequency of the beam particle with Lorentz factors  $\gamma$  and  $\beta$ . Although this impedance is capacitive, however, it appears in the form of a negative inductance. The corresponding wake function is

$$W_0'(z) = -\delta'(z/v) \frac{\omega}{\omega_0} \frac{Z_0}{2\gamma^2\beta} \left( \frac{1}{2} + 2 \ln \frac{b}{a} \right). \quad (1.15)$$

An important impedance is that of a resonant cavity. Near the resonant frequency  $\omega_r/(2\pi)$ , the longitudinal and transverse impedances can be derived from a  $RLC$ -parallel circuit:

$$Z_0^\parallel(\omega) = \frac{R_{0s}}{1 + iQ \left( \frac{\omega_r}{\omega} - \frac{\omega}{\omega_r} \right)}, \quad (1.16)$$

$$Z_1^\perp(\omega) = \frac{c}{\omega} \frac{R_{1s}}{1 + iQ \left( \frac{\omega_r}{\omega} - \frac{\omega}{\omega_r} \right)}. \quad (1.17)$$

Another example is the longitudinal impedance for a length  $\ell$  of the resistive beam pipe:

$$Z_0^\parallel(\omega) = [1 - i \text{sgn}(\omega)] \frac{\ell}{2\pi b \sigma_c \delta_{\text{skin}}}, \quad (1.18)$$

where  $b$  is the radius of the cylindrical beam pipe,  $\sigma_c$  the conductivity of the pipe wall,

$$\delta_{\text{skin}} = \sqrt{\frac{2c}{Z_0 \mu_r \sigma_c |\omega|}}, \quad (1.19)$$

the skin depth at frequency  $\omega/(2\pi)$ , and  $\mu_r$  the relative magnetic permeability of the pipe wall. The transverse impedance is

$$Z_1^\perp(\omega) = [1 - i \text{sgn}(\omega)] \frac{\ell c}{\pi \omega b^3 \sigma_c \delta_{\text{skin}}}, \quad (1.20)$$

and is related to the longitudinal impedance by

$$Z_1^\perp(\omega) = \frac{2c}{b^2 \omega} Z_0^\parallel(\omega). \quad (1.21)$$

---

<sup>‡</sup>Here the space-charge force seen by the the beam has been averaged over the cross section of the beam. If we consider instead the force seen only by the beam particles at the beam axis, the first factor  $\frac{1}{2}$  in the bracket becomes 1.

The above relation has been used very often to estimate the transverse impedance from the longitudinal. However, we should be aware that this relation holds only for resistive impedances of a cylindrical beam pipe. The monopole longitudinal impedance and the dipole transverse impedance belong to different azimuthals; therefore they should not be related.

## EXERCISES

- 1.1. Prove the properties of the impedances in Eqs. (1.9)-(1.12).
- 1.2. Using a *RLC*-parallel circuit, derive the longitudinal impedance in Eq. (1.16) by identifying  $R_{0s} = R$ ,  $\omega_r = 1/\sqrt{LC}$ , and  $Q = R\sqrt{C/L}$ . Then show that the wake function is  $W_0^{\parallel} = 0$  for  $z < 0$ , and for  $z > 0$ ,

$$W_0(z) = \frac{\omega_r R_s}{Q} e^{-\alpha z/v} \left[ \cos \frac{\bar{\omega} z}{v} - \frac{\alpha}{\bar{\omega}} \sin \frac{\bar{\omega} z}{v} \right], \quad (1.22)$$

with  $\alpha = \omega_r/(2Q)$  and  $\bar{\omega} = \sqrt{\omega_r^2 - \alpha^2}$ .

- 1.3. Show that the wake functions corresponding to the longitudinal resistive wall impedance of Eq. (1.18) and the transverse resistive wall impedance of Eq. (1.20) are, respectively,

$$W_0'(z) = -\frac{\ell}{4\pi b|z|^{1/2}} \sqrt{\frac{Z_0 \mu_r}{\pi \sigma_c}}, \quad (1.23)$$

$$W_1(z) = -\frac{\ell}{\pi b|z|^{3/2}} \sqrt{\frac{Z_0 \mu_r}{\pi \sigma_c}}. \quad (1.24)$$

The above are only approximates and are valid for  $b\chi^{1/3} \ll z \ll b/\chi$ , where  $\chi = 1/(b\sigma_c Z_0)$ .

## 2 LONGITUDINAL PHASE SPACE

### 2.1 EQUATIONS OF MOTION

To measure the charge distribution in a bunch, we choose a fixed reference point  $s_0$  along the ring and put a detector there. A particle in a bunch is characterized longitudinally by  $\tau$ , the time it arrives at  $s_0$  ahead of the synchronous particle. We record the amount of charge arriving when the time advance is between  $\tau$  and  $\tau + d\tau$ . The result is  $e\rho(\tau)d\tau$ , where  $\rho(\tau)$  is a measure of the particle distribution and  $e$  is the particle charge. The actual linear particle density per unit length is  $\lambda(\tau) = \rho(\tau)/v$ , where  $v$  is the velocity of the synchronous particle. Note that this charge distribution is measured at a fixed point but at different times. Therefore, it is *not* a periodic function of  $\tau$ . In one turn, the change in time advance is

$$\Delta\tau = -\eta T_0 \delta, \quad (2.1)$$

where  $\delta$  is the fractional momentum offset of the particle,  $T_0$  the revolution period of the synchronous particle, and  $\eta$  the slip factor. The negative sign comes about because the period of a higher-momentum particle is larger above transition ( $\eta > 0$ ) and therefore its time of arrival slips. During that turn, the energy gained by the particle relative to the synchronous particle is

$$\Delta E = eV_{\text{rf}}(\sin \phi - \sin \phi_s) - (U - U_s) - C(\langle F_0^{\parallel} \rangle - \langle F_{0s}^{\parallel} \rangle), \quad (2.2)$$

where the subscript  $s$  stands for synchronous particle, and  $C$  is the ring circumference. The first term on the right is the sinusoidal rf voltage and the second term is the radiation energy. The third is the wake force defined in the previous section due to all beam particles ahead; it can therefore be written as

$$\langle F_0^{\parallel}(\tau) \rangle = \frac{e^2}{C} \int_0^{\infty} d\tau' \rho(\tau') W_0'(\tau' - \tau) . \quad (2.3)$$

Notice that we have written, for convenience, the wake function as a function of time advance. The  $\langle F_{0s}^{\parallel} \rangle$  is the wake force on the synchronous particle. It is a constant energy loss, which is compensated by suitably choosing the synchronous phase  $\phi_s$ .

The two equations of motion are related because the momentum spread is related to the energy spread by  $\delta = \Delta E / (\beta^2 E_0)$ , and the rf phase seen is related to the time advance,

$$\phi - \phi_s = -h\omega_0\tau , \quad (2.4)$$

where  $h$  is the rf harmonic,  $E_0$  and  $\omega_0/(2\pi)$  are the energy and revolution frequency of the synchronous particle. The negative sign on the right-hand side of Eq. (2.4) comes about because when the particle arrives earlier or  $\tau > 0$ , it sees a rf phase *earlier* than the synchronous phase  $\phi_s$ . To simplify the mathematics, a continuous independent variable is needed instead of the discrete turn number. Time is not a good variable here because it is complicated by synchrotron motion and the acceleration process. We choose instead  $s$ , the distance along the closed orbit of the synchronous particle. With  $\tau$  and  $\Delta E$  as the canonical variables<sup>†</sup>, the equations of motion for a particle in a small bunch become

$$\frac{d\tau}{ds} = -\frac{\eta}{v\beta^2 E_0} \Delta E , \quad (2.5)$$

$$\frac{d\Delta E}{ds} = -\frac{eh\omega_0^2 V_{\text{rf}} \cos \phi_s}{2\pi v} \tau - \frac{U - U_s}{C} - \langle F_0^{\parallel} \rangle . \quad (2.6)$$

If the radiation energy is neglected, the two equations of motion are derivable from the Hamiltonian

$$H = -\frac{\eta}{2v\beta^2 E_0} (\Delta E)^2 + \frac{eh\omega_0^2 V_{\text{rf}} \cos \phi_s}{4\pi v} \tau^2 + V(\tau) , \quad (2.7)$$

where

$$V(\tau) = \frac{e^2}{C} \int_0^{\tau} d\tau'' \int_{\tau''}^{\infty} d\tau' \rho(\tau') W_0'(\tau' - \tau) . \quad (2.8)$$

Substituting for the unperturbed small-amplitude synchrotron angular frequency

$$\omega_{0s} = \omega_0 \sqrt{-\frac{\eta h V_{\text{rf}} \cos \phi_s}{2\pi \beta^2 E_s}} , \quad (2.9)$$

the Hamiltonian becomes

$$H = -\frac{\eta}{2v\beta^2 E_0} (\Delta E)^2 - \frac{\omega_{0s}^2 \beta^2 E_0}{2\eta v} \tau^2 + V(\tau) . \quad (2.10)$$

## 2.2 VLASOV EQUATION

We would like to describe the collective behavior of a multi-particle system under the influence of electromagnetic forces. When collisions are neglected, the Vlasov equation or the Liouville theorem [2] is

---

<sup>†</sup>This set of canonical variables should not be used if the accelerator is ramping.

the right candidate. It states that if we follow the motion of a representative particle in the longitudinal or  $\tau$ - $\Delta E$  phase space, the density of particles in its neighborhood is constant. In other words, the distribution of particles  $\psi(\tau, \Delta E; s)$  moves in the longitudinal phase space like an incompressible fluid. Mathematically, the Vlasov equation reads

$$\frac{d\psi}{ds} = \frac{\partial\psi}{\partial s} + \frac{d\tau}{ds} \frac{\partial\psi}{\partial\tau} + \frac{d\Delta E}{ds} \frac{\partial\psi}{\partial\Delta E} = 0. \quad (2.11)$$

In terms of the Hamiltonian, it becomes

$$\frac{\partial\psi}{\partial s} + [\psi, H] = 0, \quad (2.12)$$

where  $[\cdot, \cdot]$  denotes the Poisson bracket.

## EXERCISES

- 2.1. The Hamiltonian of Eq. (2.7) describes motion in the longitudinal phase space. Find the fixed points of the Hamiltonian above and below transition, and determine whether they are stable or not. The separatrices are the contours of fixed Hamiltonian values that pass through the unstable fixed points. They separate the region of libration motion (oscillatory motion) from rotation motion. Plot the separatrices.
- 2.2. The canonical variables  $\tau_0$  and  $\Delta E_0$  evaluated at ‘time’  $s = 0$  become  $\tau_1$  and  $\Delta E_1$  at an infinitesimal time  $\Delta s$  latter according to

$$\tau_1 = \tau_0 + \frac{\partial H}{\partial \Delta E} \Delta s, \quad \Delta E_1 = \Delta E_0 - \frac{\partial H}{\partial \tau} \Delta s. \quad (2.13)$$

Consider the small phase-space area element  $d\tau_0 d\Delta E_0 = J d\tau_1 d\Delta E_1$ . Show that the Jacobian  $J = 1$  to the first order of  $\Delta s$ , implying that the area surrounding a given number of particles does not change in time, which is Liouville Theorem. It is possible to prove  $J = 1$  to all orders of  $\Delta s$  using canonical transformation. See, for example, H. Goldstein, *Classical Mechanics*, Addison-Wesley, Chapter 8-3.

## 3 POTENTIAL-WELL DISTORTION

A stationary bunch distribution  $\psi$  is time-independent. Therefore we expect  $[\psi, H] = 0$ , or  $\psi$  must be a function of the Hamiltonian,

$$\psi = \psi(H). \quad (3.1)$$

For an electron bunch, because of the random quantum radiation and excitation, stationary distribution should have a Gaussian distribution in  $\Delta E$ , or

$$\psi(\tau, \Delta E) = \frac{1}{\sqrt{2\pi}\sigma_E} \exp\left(-\frac{\Delta E^2}{2\sigma_E^2}\right) \rho(\tau), \quad (3.2)$$

where  $\sigma_E$  is the rms beam energy spread determined by synchrotron radiation. Noting Eq. (3.1), we must have

$$\psi(\tau, \Delta E) \propto \exp\left(\frac{v\beta^2 E_0}{\eta\sigma_E^2} H\right). \quad (3.3)$$

Integrating over  $\Delta E$ , we finally arrive at an equation for the line density,

$$\rho(\tau) = \rho(0) \exp\left[-\left(\frac{\omega_s \beta^2 E_0}{\eta\sigma_E}\right)^2 \frac{\tau^2}{2} + \frac{e^2 \beta^2 E_0}{\eta I_0 \sigma_E^2} \int_0^\tau d\tau'' \int_{\tau''}^\infty d\tau' \rho(\tau') W_0'(\tau' - \tau)\right]. \quad (3.4)$$

This is called the *Haissinski equation* [3], where the constant  $\rho(0)$  is obtained by normalizing to the total number of particles in the bunch:

$$\int d\tau \rho(\tau) = N . \quad (3.5)$$

The solution will give a line distribution that deviates from the Gaussian form, and we call this the *potential-well distortion*. Since the rf voltage is modified, the synchrotron frequency also changes from  $\omega_{0s}/(2\pi)$  to perturbed incoherent  $\omega_s/(2\pi)$  accordingly.

For a purely resistive impedance  $Z_0^{\parallel}(\omega) = R_s$ ,  $W_0'(z) = R_s\delta(z/v)$ , the equation can be solved analytically giving the solution [4]

$$\rho(\tau) = \frac{\sqrt{2/\pi} e^{-\tau^2/(2\sigma_\tau^2)}}{\alpha_R \sigma_\tau \{ \coth(\alpha_R N/2) - \text{erf}[\tau/(\sqrt{2}\sigma_\tau)] \}} , \quad (3.6)$$

where  $\sigma_\tau = |\eta|\sigma_E/(\beta^2\omega_s E_0)$ .  $\alpha_R = e^2\beta^2 E_0 R_s/(\eta T_0 \sigma_E^2)$ , and  $\text{erf}(x) = (2/\sqrt{\pi}) \int_0^x e^{-t^2} dt$  is the error function. For a weak beam with  $|\alpha_R|N \lesssim 1$ , the peak beam density occurs at

$$\tau = \frac{\alpha_R N}{\sqrt{2\pi}} \sigma_\tau . \quad (3.7)$$

This peak moves forward above transition and backward below transition as the beam intensity increases. This effect comes from the parasitic loss of the beam.

When the longitudinal impedance is purely inductive,  $W_0'(z) = L\delta'(z/v)$ , the Haissinski equation becomes

$$\rho(\tau) = k e^{-\tau^2/(2\sigma_\tau^2) - \alpha_L \rho(\tau)} , \quad (3.8)$$

where  $k$  is a positive constant and  $\alpha_L = e^2\beta^2 E_0 L/(\eta T_0 \sigma_E^2)$ . Thus,  $\rho e^{\alpha_L \rho}$  is an even function of  $\tau$ , and it appears that the distorted distribution  $\rho$  is also an even function of  $\tau$ . The line distribution will be left-right symmetric. Thus, the reactive part of the impedance will either lengthen or shorten the bunch, while the resistive part will cause the bunch to lean forward or backward. When  $|\alpha_L|N \lesssim 1$ , we can iterate,

$$\rho \approx k e^{-\tau^2/(2\sigma_\tau^2)} \left( 1 - k \alpha_L e^{-\tau^2/(2\sigma_\tau^2)} \right) . \quad (3.9)$$

Thus for  $\alpha_L > 0$  the effective rms bunch length will be larger than  $\sigma_\tau$ . This is the situation of either a repulsive inductive impedance force above transition or a repulsive capacitive force ( $L < 0$ ) below transition. On the other hand, for an attractive inductive force below transition or an attractive capacitive force above transition,  $\alpha_L < 0$  and the bunch will be shortened.

An easier way to compute the bunch length distorted by the reactive impedance is to consider the elliptic phase space distribution

$$\psi(\tau, \Delta E) = \frac{3N|\eta|\sqrt{\kappa}}{2\pi\beta^2\omega_s E_0 \hat{\tau}_0^3} \sqrt{\hat{\tau}_0^2 - \left( \frac{\eta}{\beta^2\omega_s E_0} \right)^2 \Delta E^2 - \kappa\tau^2} . \quad (3.10)$$

This distribution has a constant maximum energy spread of

$$\widehat{\Delta E} = \frac{\beta^2\omega_s E_0 \hat{\tau}_0}{|\eta|} , \quad (3.11)$$

which is determined by synchrotron radiation, while the half width of the bunch

$$\hat{\tau} = \frac{\hat{\tau}_0}{\sqrt{\kappa}} \quad (3.12)$$

is determined by the parameter  $\kappa$ . This distribution when integrated over  $\Delta E$  gives the normalized parabolic line distribution

$$\rho(\tau) = \frac{3N\sqrt{\kappa}}{4\hat{\tau}_0^3} (\hat{\tau}_0^2 - \kappa\tau^2) . \quad (3.13)$$

With the reactive wake function  $W'_0(z) = L\delta'(z/v)$ , the Hamiltonian of Eq. (2.7) can therefore be written as a quadratic in  $\Delta E$  and  $\tau$ :

$$H = -\frac{\eta}{2v\beta^2 E_0} (\Delta E)^2 - \frac{\omega_s^2 \beta^2 E_0}{2\eta v} \tau^2 - \frac{e^2 L}{C} \rho(\tau) \quad (3.14)$$

$$= \frac{\omega_s^2 \beta^2 E_0}{2\eta v} \left[ -\left( \frac{\eta}{\beta^2 \omega_s E_0} \right)^2 \Delta E^2 - \tau^2 (1 - D\kappa^{3/2}) \right] , \quad (3.15)$$

where

$$D = \frac{3e^2 N \eta v L}{2\omega_s^2 \beta^2 E_0 C \hat{\tau}_0^3} . \quad (3.16)$$

To be self-consistent, the expression of  $\psi$  in Eq. (3.10) must be a function of the Hamiltonian. Comparing Eq. (3.10) with Eq. (3.15), we arrive at

$$\kappa = 1 - D\kappa^{3/2} \quad (3.17)$$

or

$$\left( \frac{\hat{\tau}}{\hat{\tau}_0} \right)^3 = \left( \frac{\hat{\tau}}{\hat{\tau}_0} \right) + D . \quad (3.18)$$

This cubic can be solved by iteration. First we put  $\hat{\tau}/\hat{\tau}_0 = 1$  on the right side. If  $D > 0$ , we find  $\hat{\tau}/\hat{\tau}_0 > 1$  or the bunch is lengthened. If  $D < 0$ , it is shortened. The former corresponds to either an inductive force above transition or a capacitive force below transition. The latter corresponds to either an inductive force below transition or a capacitive force above transition.

For a proton bunch, the energy spread is also modified but the bunch area remains constant. The phase-space distribution has to be rewritten as

$$\psi(\tau, \Delta E) = \frac{3N|\eta|}{2\pi\beta^2\omega_s E_0 \hat{\tau}_0^3} \sqrt{\hat{\tau}_0^2 - \frac{1}{\kappa} \left( \frac{\eta}{\beta^2 \omega_s E_0} \right)^2 \Delta E^2 - \kappa\tau^2} . \quad (3.19)$$

Now we have

$$\hat{\tau} = \frac{\hat{\tau}_0}{\sqrt{\kappa}} \quad \text{and} \quad \widehat{\Delta E} = \sqrt{\kappa} \widehat{\Delta E}_0 . \quad (3.20)$$

Again comparing with the Hamiltonian, we arrive at the quartic equation

$$\left( \frac{\hat{\tau}}{\hat{\tau}_0} \right)^4 = 1 + D \left( \frac{\hat{\tau}}{\hat{\tau}_0} \right) . \quad (3.21)$$

## EXERCISES

3.1. Transform the Haissinski equation (3.4) according to the following:

(1) Notice that the integral over  $\tau''$  can be rewritten as

$$\int_0^\tau d\tau'' \rightarrow - \int_\tau^\infty d\tau'' , \quad (3.22)$$

where the extra constant can be absorbed into the normalization constant  $\rho(0)$  which we rename by  $\xi$ .

(2) The integration in the  $\tau'$ - $\tau''$  space is in the  $0^\circ$  to  $45^\circ$  quadrant between the lines  $\tau'' = \tau$  and  $\tau'' = \tau'$ . Translate the  $\tau'$  and  $\tau''$  axes so that the region of integrated is now between the  $\tau'$ -axis and the  $45^\circ$  line  $\tau'' = \tau'$ .

(3) Integrate over  $\tau''$  first from 0 to  $\tau'$ ; then integrate over  $\tau'$ .

(4) Change the variable  $\tau''$  to  $\tau' + \tau''$ . Now the Haissinsky equation takes the more convenient form

$$\rho(\tau) = \xi \exp \left[ - \left( \frac{\omega_s \beta^2 E_0}{\eta \sigma_E} \right)^2 \frac{\tau^2}{2} - \frac{e^2 \beta^2 E_0}{\eta T_0 \sigma_E^2} \int_0^\infty d\tau' \rho(\tau + \tau') \int_0^{\tau'} d\tau'' W_0'(\tau'') \right]. \quad (3.23)$$

Notice that  $\rho(\tau)$  on the left side only depends on the  $\rho$  on the right side evaluated in front of  $\tau$ . We can therefore solve for  $\rho$  at successive slides of the bunch by assigning zero to  $\rho$  at the very first slide (the head) and some value to the constant  $\xi$ . The value of  $\xi$  is varied until the proper normalization of  $\rho$  is obtained.

- 3.2. The bunch in the Fermilab Tevatron contains  $N = 2.7 \times 10^{11}$  proton has a designed half length of  $\tau = 2.75$  ns. The ring main radius is  $R = 1$  km and the slip factor is  $\eta = 0.0028$  at the incident energy of  $E_0 = 150$  GeV. The rf harmonic is  $h = 1113$  and the rf voltage is  $V_{rf} = 1.0$  MV. Assume a broad-band impedance centered at  $\omega_r/(2\pi) \approx 3$  GHz, quality factor  $Q = 1$ , and shunt impedance  $R_s = 250$  k $\Omega$ .

(a) Show that the frequencies that the bunch samples are much less than the resonant frequency of the broad-band, so that the asymmetric beam distortion driven by  $\text{Re } Z_0^{\parallel}$  can be neglected.

(b) Using only the inductive part of the impedance at low frequencies, compute from Eq. (3.21) the equilibrium bunch length as a result of potential-well distortion.

(c) Electron bunches are usually very short. If an electron bunch of rms bunch length 2 cm is put into the Tevatron, show that its spectrum will sample the resonant peak of  $\text{Re } Z_0^{\parallel}$  and thus suffer asymmetric distortion. Verify this by substituting the data into Eq. (3.6).

- 3.3. From Eq. (3.18) for an electron bunch, show that there are two solutions for the perturbed bunch length due to distortion by a capacitive impedance when  $-2/3^{3/2} < D < 0$ . Which one is physical? When  $D < -2/3^{3/2}$ , there is no solution. At this critical situation, the bunch shortening ratio is  $1/3^{-1/2}$ .

## 4 LONGITUDINAL MICROWAVE INSTABILITY

The equation of motion for the longitudinal coordinate  $\tau$  of a particle can be obtained from Eqs. (2.5) and (2.6):

$$\frac{d^2\tau}{ds^2} + \frac{\omega_s^2}{v^2}\tau = \frac{\eta}{v\beta^2 E_0} \langle F_0^{\parallel}(\tau) \rangle. \quad (4.1)$$

For a reactive wake function  $W_0'(z) = L\delta'(z/v)$ , it reduces to

$$\frac{d^2\tau}{ds^2} + \frac{\omega_s^2}{v^2}\tau = -\frac{e^2\eta L}{v\beta^2 C E_0} \rho'(\tau). \quad (4.2)$$

For a rather long and uniform bunch, the slope of the linear distribution is mostly zero. Now suppose a small bump appears in the linear density with distribution  $\rho(\tau)$ . The front of the bump has  $\rho'(\tau) < 0$  and the rear  $\rho'(\tau) > 0$ . For an inductive wake ( $L > 0$ ) above transition ( $\eta > 0$ ) or a capacitive wake below

transition, particles at the front of the bump accelerate and those at the rear decelerate resulting in the smoothing out of the bump. However, for an inductive wake below transition or a capacitive wake above transition, particles at the front of the bump decelerate and those at the rear accelerate, thus enhancing the bump. In other word, the situation is unstable against small nonuniformity in the linear distribution. In order for the bump to grow, the growth rate must be faster than phase-drifting rate coming from the momentum spread of the beam. This damping process is called *Landau damping* [5]. For a bunch, the growth must be faster than synchrotron frequency otherwise the bump will be smeared out. Also since the size of the bump must be less than the length of the bunch, the impedance driving the instability must have a wavelength less than the length of the bunch. This growth at high frequencies is called *microwave instability*.

## 4.1 DISPERSION RELATION

For the dispersion relation governing microwave instability, we follow closely the derivation of Chao [6]. Consider a coasting beam, i.e.,  $\omega_s = 0$ , with the unperturbed phase-space distribution

$$\psi_0(\Delta E) = \frac{N}{T_0} f_0(\Delta E) , \quad (4.3)$$

where  $f_0(\Delta E)$  is normalized to unity when integrated over  $\Delta E$ . Since the line distribution is uniform, it does not depends on the location  $s$  along the ring. This stationary distribution is perturbed by an infinitesimal longitudinal density wave which we postulate to have the ansatz

$$\psi_1(s, t, \Delta E) = \hat{\psi}_1(\Delta E) e^{ins/R - i\Omega t} , \quad (4.4)$$

where  $n$  is a nonzero integer,  $R$  the mean radius of the ring, and  $\Omega/(2\pi)$  the collective frequency of oscillation to be determined. When integrated over  $\Delta E$ , we get the perturbation line density

$$\rho_1(s, t) = \hat{\rho}_1 e^{ins/R - i\Omega t} . \quad (4.5)$$

A particle at position  $s$  and time  $t$  sees a wake force due to all beam particles that pass  $s$  at a time  $z/v$  earlier. This force can be expressed as

$$\langle F_0^{\parallel}(s, t) \rangle = \frac{e^2}{C} \int_0^{\infty} \frac{dz}{v} \rho_1(s, t - z/v) W_0'(z) = \frac{e^2}{C} \rho_1(s, t) Z_0^{\parallel}(\Omega) , \quad (4.6)$$

where  $Z_0^{\parallel}(\Omega)$  is the longitudinal impedance of the vacuum chamber evaluated at the collective frequency. The particle energy will be perturbed according to the equation of motion

$$\frac{d\Delta E(s, t)}{ds} = -\frac{e^2}{C} Z_0^{\parallel}(\Omega) \hat{\rho}_1 e^{ins/R - i\Omega t} . \quad (4.7)$$

The energy change will induce a drift in the time advance

$$\frac{d\tau(s, t)}{ds} = -\frac{\eta \Delta E(s, t)}{v \beta^2 E_0} . \quad (4.8)$$

Note that for a particle,  $s = s_0 + vt$ , where  $s_0$  is the particle location at  $t = 0$ . Eliminating  $t$ , the equations can be integrated readily to give,

$$\Delta E(s, t) = -i \frac{e^2 Z_0^{\parallel}(\Omega)}{T_0} \frac{\hat{\rho}_1 e^{ins/R - i\Omega t}}{\Omega - n\omega_0} , \quad (4.9)$$

$$\tau(s, t) = -\frac{e^2 \eta Z_0^{\parallel}(\Omega)}{\beta^2 E_0 T_0} \frac{\hat{\rho}_1 e^{ins/R - i\Omega t}}{(\Omega - n\omega_0)^2} , \quad (4.10)$$

where we have retained only the modifications in  $\Delta E(s, t)$  and  $\tau(s, t)$  which reflect the presence of the impedance. There is neglected in Eq. (4.9) a constant term which corresponds to the energy spread of the particle in the absence of the impedance. Also neglected is a constant term in Eq. (4.10) that corresponds to the time advance drift as a result of the unperturbed energy spread of the particle. Therefore, particles at locations between  $s$  and  $s + ds$  in the unperturbed beam  $\psi_0$  at time  $t$  are the same particles at locations between  $s + v\tau(s, t)$  and  $s + ds + v\tau(s + ds, t)$  in the perturbed distribution  $\psi_0 + \psi_1$  at time  $t$ . In other words,

$$\psi_0(\Delta E) ds d\Delta E = [\psi_0(\Delta E) + \psi_1(s, t, \Delta E)] \{ [s + ds + v\tau(s + ds, t)] - [s + v\tau(s, t)] \} . \quad (4.11)$$

We get

$$\psi_1(s, t, \Delta E) = -v\psi_0(\Delta E) \frac{\partial \tau(s, t)}{\partial s} , \quad (4.12)$$

$$= \frac{ie^2 N v \eta n Z_0^{\parallel}(\Omega)}{\beta^2 E_0 T_0^2} \frac{f_0(\Delta E)}{(\Omega - n\omega_0)^2} \hat{\rho}_1 e^{ins/R - i\Omega t} . \quad (4.13)$$

Canceling the exponential on both side, we obtain

$$\hat{\psi}_1(\Delta E) = \frac{ieI_0 \eta n Z_0^{\parallel}(\Omega) \omega_0^2}{2\pi \beta^2 E_0} \frac{f_0(\Delta E)}{(\Omega - n\omega_0)^2} \hat{\rho}_1 , \quad (4.14)$$

where  $I_0 = eN/T_0$  is the average beam current. Recalling that  $\hat{\psi}_1(\Delta E)$  is normalized to  $\hat{\rho}_1$ , integrating over  $\Delta E$  on both side, we arrive at the dispersion relation

$$1 = \frac{ieI_0 \eta n Z_0^{\parallel}(\Omega)}{2\pi \beta^2 E_0} \int \frac{\omega^2 f_0(\Delta E)}{(\Omega - n\omega)^2} d\Delta E , \quad (4.15)$$

where  $\omega$  has been used to denote the various revolution angular frequencies of the beam particles while  $\omega_0$  has been reserved for the revolution angular frequency of the on-energy particle. An immediate conclusion of Eq. (4.15) is that our ansatz for  $\psi_1$  in Eq. (4.4) is correct and the revolution harmonics are decoupled. If there is no energy spread, the collective frequency can be solved easily. Above transition or  $\eta > 0$ ,

$$\Omega = n\omega_0 + \sqrt{\frac{eI_0 \eta n}{2\pi \beta^2 E_0}} \sqrt{i \operatorname{Re} Z_0^{\parallel}(\Omega) - \operatorname{Im} Z_0^{\parallel}(\Omega) \omega_0} , \quad (4.16)$$

of which the positive imaginary part is the growth rate. We see that above transition there is no growth only when  $Z_0^{\parallel}$  is purely inductive, as postulated at the beginning of the discussion. For a low-energy machine, the space-charge impedance per harmonic is frequency independent and rolls off only at very high frequencies. Therefore above transition, the growth rate is directly proportional to  $n$  or frequency. This is the source of negative-mass instability for a proton machine just above transition.

Now let us consider a realistic beam that has an energy spread. Since  $\omega$  is a function of the energy offset  $\Delta E$ , define a revolution frequency distribution  $g_0(\omega)$  for the unperturbed beam such that

$$g_0(\omega) d\omega = f_0(\Delta E) d\Delta E . \quad (4.17)$$

Substituting into Eq. (4.14) and integrating by part, we obtain

$$1 = -\frac{ieI_0 \eta Z_0^{\parallel}(\Omega)}{2\pi \beta^2 E_0} \int \frac{\omega^2 g'_0(\omega)}{\Omega - n\omega} d\omega . \quad (4.18)$$

Given the frequency distribution  $g_0(\omega)$  of the unperturbed beam and the impedance  $Z_0^{\parallel}$  of the ring at roughly  $n\omega_0$ , the collective frequency can be solved from the dispersion equation. For a Gaussian distribution, the integral is related to the complex error function, so that an analytic solution can be written down. For other distributions, one has to resort to numerical method. For a given growth rate or  $\mathcal{I}m \Omega$ , we perform the integral for various values of  $\mathcal{R}e \Omega$  and read off  $\mathcal{R}e Z_0^{\parallel}$  and  $\mathcal{I}m Z_0^{\parallel}$  from the dispersion equation. Thus, we can plot a contour in the  $\mathcal{R}e Z_0^{\parallel}$ - $\mathcal{I}m Z_0^{\parallel}$  plane corresponding to a certain growth rate. This plot for the Gaussian distribution below transition is shown in Fig. 3. What are plotted is the real part  $U'$  and imaginary part  $V'$  of

$$U' + iV' = \frac{eI_0\beta^2(Z_0^{\parallel}/n)}{|\eta|E_0(\Delta E/E)_{\text{FWHM}}^2} \quad (4.19)$$

at fixed growth rates. From outside to inside, the contours in the figure correspond to growth rates 0.5 to  $-0.5$  in steps of  $-0.1$  in units of HWHM of the frequency spread, where negative values imply damping.

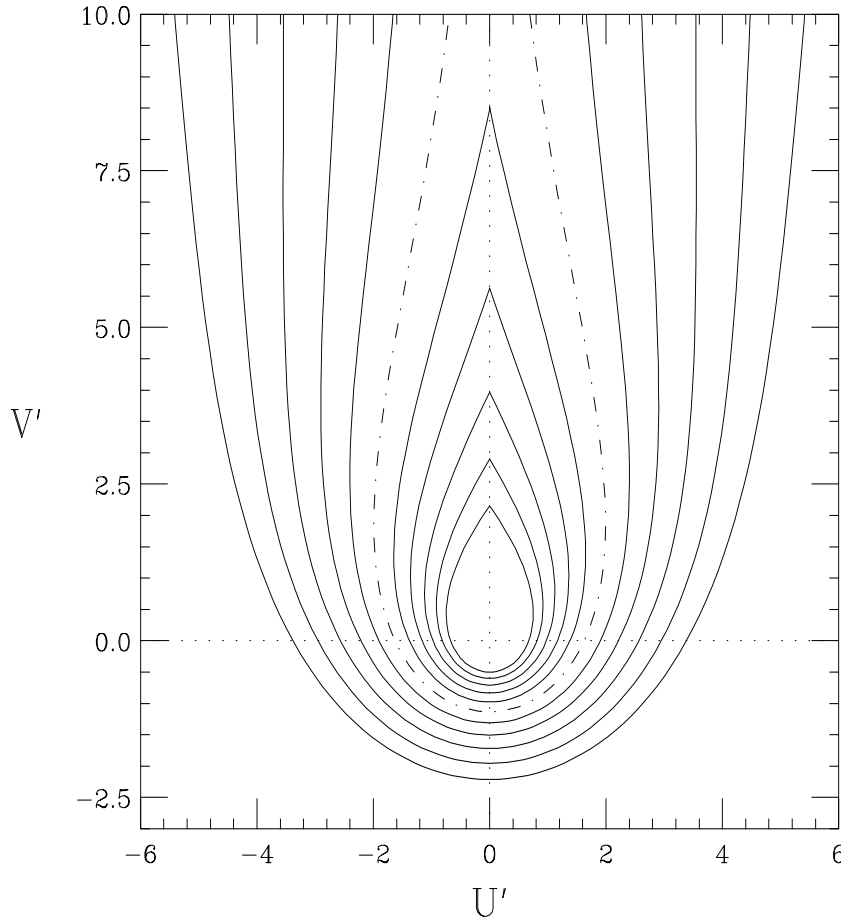


Figure 3: The growth contours for a Gaussian distribution in revolution frequency below transition. The abscissa  $U'$  and ordinate  $V'$  are, respectively, real and imaginary parts of  $eI_0\beta^2(Z_0^{\parallel}/n)/[|\eta|E_0(\Delta E/E)_{\text{FWHM}}^2]$ . From outside to inside, the contours correspond to growth rates 0.5 to  $-0.5$  in steps of  $-0.1$  in units of HWHM of the frequency spread, where negative values imply damping. The contour corresponding to the stability threshold is drawn in dot-dashes and the area inside it is stable.

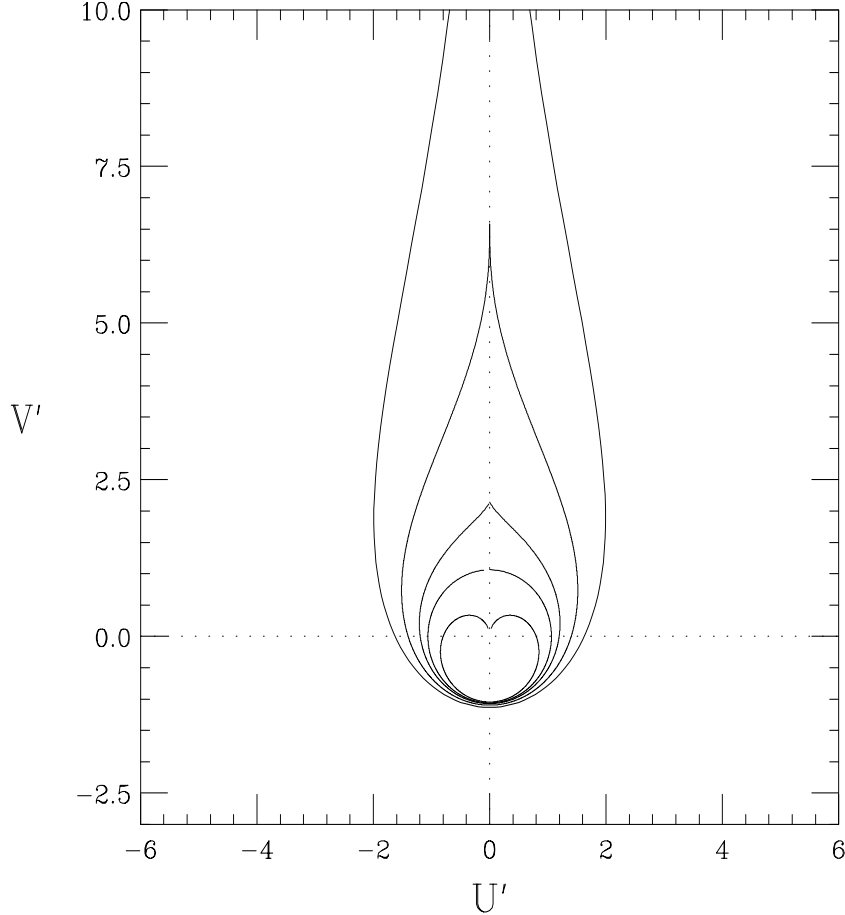


Figure 4: The stability contours for different frequency distribution below transition. The abscissa  $U'$  and ordinate  $V'$  are, respectively, real and imaginary parts of  $eI_0\beta^2(Z_0^{\parallel}/n)/[|\eta|E_0(\Delta E/E)_{\text{FWHM}}^2]$ . From inside to outside, they correspond to unperturbed revolution frequency distribution  $f(x) = \frac{3}{4}(1-x^2)$ ,  $\frac{8}{3\pi}(1-x^2)^{3/2}$ ,  $\frac{15}{16}(1-x^2)^2$ ,  $\frac{315}{32}(1-x^2)^4$ , and  $\frac{1}{\sqrt{2\pi}}e^{-x^2/2}$ . Note that all contours cut the  $V'$ -axis at about  $-1$ .

The contour corresponding to the stability threshold is drawn in dot-dashes and the area inside it is stable. Note that the positive  $V'$ -axis is a cut and those damping contours continue into other Riemann sheets after passing through the cut. Therefore, for each  $(U', V')$  outside the stability region bounded by the dot-dashed curve, there can also be one or more stable solutions. However, since there is at least one unstable solution, this outside region is termed unstable.

Obviously, these contours depend on the distribution  $g_0(\omega)$  assumed. In Fig. 4, we plot the stability contours for various frequency distributions below transition. They are for frequency distributions, from inside to outside,  $f(x) = \frac{3}{4}(1-x^2)$ ,  $\frac{8}{3\pi}(1-x^2)^{3/2}$ ,  $\frac{15}{16}(1-x^2)^2$ ,  $\frac{315}{32}(1-x^2)^4$ , and  $\frac{1}{\sqrt{2\pi}}e^{-x^2/2}$ . The innermost one is the parabolic distribution with discontinuous density slopes at the edges and we see that the stability contour curves towards the origin in the positive  $V'$  region. The contour next to it corresponds to continuous density slopes at the edges and it does not dip downward in the positive  $V'$  region. As the edges become smoother or with higher derivatives that are continuous, the contour shoots up higher in the upper half

plane. For all distributions with a finite spread, the contours end with finite values at the positive  $V'$ -axis. For the Gaussian distribution which has infinite spread and continuous derivatives up to infinite orders, the contour will only approach the positive  $V'$ -axis without intersecting it.

We note in Fig. 4 that, regardless the form of distribution, all contours cut the negative  $V'$ -axis at  $\sim -1$ . Therefore, it is reasonable to approximate the stability region by a unit circle in the  $U'$ - $V'$  plane, so that a stability criterion can be written analytically. This is the *Keil-Schnell criterion* which reads [7]

$$\left| \frac{Z_0^{\parallel}}{n} \right| < F \frac{|\eta| E_0}{e I_0 \beta^2} \left( \frac{\Delta E}{E_0} \right)_{\text{FWHM}}^2, \quad (4.20)$$

where  $F$  is a distribution-dependent form factor and is equal to the negative  $V'$ -intersection of the contour. For all the distributions discussed here,  $F \approx 1$ . (See Exercise 4.1 below).

For a bunch beam, if the disturbance has a wavelength much less than the bunch length, we can view the bunch locally as a coasting beam. Boussard suggested to apply the same Keil-Schnell stability criterion to a bunch beam by replacing the coasting beam current  $I_0$  with the peak current  $I_{\text{peak}}$  of the bunch. Krinsky and Wang [8] performed a vigorous derivation of the microwave stability limit for a bunch beam with a Gaussian energy spread and found the stability criterion

$$\left| \frac{Z_0^{\parallel}}{n} \right| < \frac{2\pi |\eta| E_0}{e I_{\text{peak}} \beta^2} \left( \frac{\Delta E}{E_0} \right)_{\text{rms}}^2. \quad (4.21)$$

Comparing with Eq. (4.20), the Krinsky-Wang criterion corresponds to the Keil-Schnell criterion with a form factor of  $\pi/(4 \ln 2) = 1.133$ , which is exactly the negative  $V'$ -intersect (see Exercise 4.1.)

## 4.2 LANDAU DAMPING

Keil-Schnell Criterion can be written as

$$n\omega_0 \sqrt{\frac{e|\eta||Z_0^{\parallel}|/n|I_0}{2\pi\beta^2 E_0}} < n\omega_0 \sqrt{\frac{F}{2\pi} \frac{|\eta|\Delta E|_{\text{FWHM}}}{\beta^2 E_0}}. \quad (4.22)$$

The left side is the growth rate as discussed in Eq. (4.16) with  $I_0$  replaced by  $I_{\text{peak}}$  in the case of a bunch. The right side can therefore be considered as the Landau damping rate coming from energy spread or frequency spread. Stability is maintained if Landau damping is large enough. The theory of Landau damping is rather profound, for example, the exchange of energy between particles and waves, the mechanism of damping, the contour around the poles in Eq. (4.15), etc. The readers are referred to the papers by Landau and Jackson [5, 9], and also a very well-written chapter in Chao's book [6].

## 4.3 SELF-BUNCHING

Neglecting the effect of wake function, the Hamiltonian for particle motion can be written as

$$H = -\frac{\eta}{2v\beta^2 E_0} (\Delta E)^2 + \frac{eV_{\text{rf}}}{2\pi v h} \cos(h\omega_0\tau), \quad (4.23)$$

where the synchronous angle has been put to zero and the small-bunch approximation has been relaxed. It is easy to see that the height of the bucket is

$$\Delta E|_{\text{bucket}} = \sqrt{\frac{eE_0 V_{\text{rf}}}{\pi h |\eta|}}. \quad (4.24)$$

Keil-Schnell criterion can also be written as

$$\sqrt{\frac{eE_0 I_0 |Z_0^{\parallel}|}{\pi n |\eta|}} < \sqrt{\frac{F}{\pi \beta^2} \Delta E|_{\text{FWHM}}} . \quad (4.25)$$

Comparing with Eq. (4.24), the left side can be viewed as the height of a bucket created by an induced voltage  $I_0 |Z_0^{\parallel}|$  while the right side roughly the half full energy spread of the beam. This induced voltage will bunch the beam just as an rf voltage does. If the self-bunched bucket height is less than the half full energy spread of the beam, the bunching effect will not be visible and beam remains coasting. Otherwise, the beam breaks up into bunchlets of harmonic  $n$ , and we call it unstable. This mechanism is known as *self-bunching*.

#### 4.4 OVERSHOOT AND BUNCH LENGTHENING

When the current is above the microwave threshold, the self-bunching concept tells us that there will be an increase in energy spread of the beam. The increase continues until it is large enough to stabilize the beam again according to the Keil-Schnell criterion. For a proton beam, experimental observation indicates that there will be an overshoot. Let  $(\Delta E)_i$  be the initial energy spread which is below the threshold energy spread  $(\Delta E)_{\text{th}}$  postulated by the Keil-Schnell criterion. The final energy spread  $(\Delta E)_f$  was found to be given empirically by [10]

$$(\Delta E)_i (\Delta E)_f = (\Delta E)_{\text{th}}^2 . \quad (4.26)$$

Thus the final energy spread is always larger than the threshold energy spread. An overshoot formula similar to but not exactly the same as Eq. (4.26) has been derived by Chin and Yokoya [11].

For an electron bunch, because of the radiation damping, there is no overshooting observed. The bunch length and energy spread as functions of average bunch current are plotted schematically in Fig. 5. When the current is very small, the bunch length and energy spread correspond to their natural values as a result of the radiation damping and the rf voltage. As the bunch current increases, the effect of potential-well distortion is visible. The impedance of an electron ring is dominated by rf cavities. Since the electron bunch is much shorter than the rf wavelength, it samples the capacitive part of cavity impedance. Therefore, the bunch becomes shorter. Notice that the energy spread which is specified by radiation damping remains unchanged. As the beam current exceeds the threshold for microwave instability, self-bunching occurs increasing the energy spread to such a value that stability is again maintained. The bunch length also increases because of synchrotron oscillation. The rms energy spread  $\sigma_E$  is related to the rms bunch length  $\sigma_\tau$  by

$$\omega_s \sigma_\tau = \eta \frac{\sigma_E}{\beta^2 E_0} . \quad (4.27)$$

From the Krinsky-Wang criterion of Eq. (4.21), we obtain the bunch length at the stability threshold,

$$\sigma_\tau = \left( \frac{e^2 N \eta \beta^2}{\sqrt{2\pi} E_0 \omega_s^2} \frac{Z_0^{\parallel}}{n} \right)^{1/3} . \quad (4.28)$$

Therefore, the bunch length depends on only one parameter

$$\xi = \frac{\eta I_b}{\nu_s^2 E_0} , \quad (4.29)$$

where  $I_b$  is the average beam current of the bunch and  $\nu_s = \omega_s / \omega_0$  is the synchrotron tune. This scaling law was first derived by Chao and Gareyte [12] and has been verified experimentally. Using the concept of mode-coupling, Chao and Gareyte derived a more general bunch length formula (see Section 9 on mode-coupling

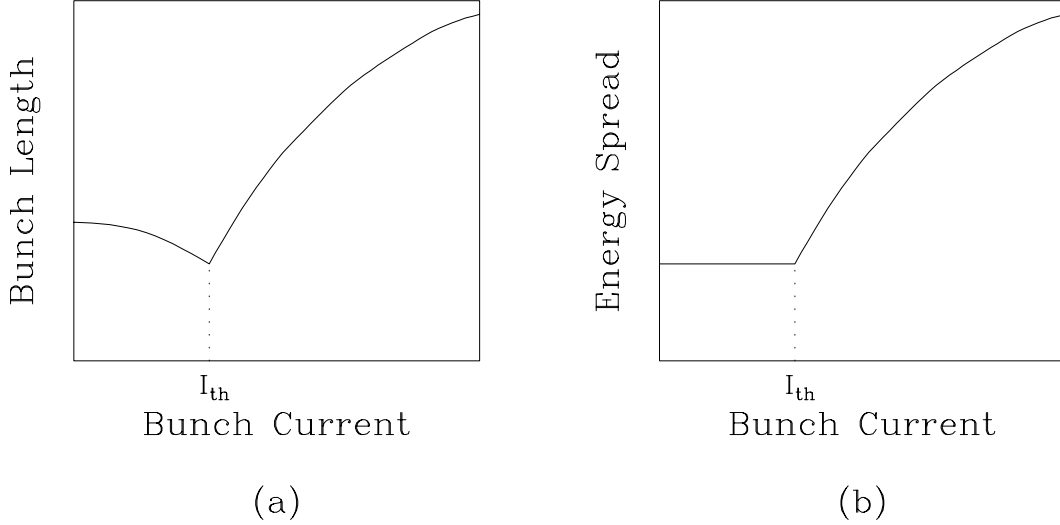


Figure 5: Both the bunch length and energy spread begin to grow after the bunch current exceeds its microwave instability threshold  $I_{th}$ . (a) The bunch length starts with its natural value at zero current and becomes shortened due to the capacitive potential-well distortion. (b) Below the instability threshold, the energy spread is always at its natural value unaffected by the effect of potential-well distortion.

below)

$$\sigma_{\tau} \propto \xi^{1/(2+a)} \quad (4.30)$$

when the part of the impedance sampled by the bunch behaves like

$$Z_0^{\parallel} \propto \omega^a . \quad (4.31)$$

The bunch length formula of Eq. (4.28) corresponds to  $a = 1$ , or a broad-band impedance at low frequency. This will be the situation for a proton machine, where the impedance rolls off around or above the cutoff frequency and the proton bunch has a length much longer than beam pipe radius and therefore samples the impedance at frequencies well below cutoff. For an electron machine, the impedance which is dominated by the rf cavities rolls off at much lower frequencies. The electron bunch which is usually short will therefore samples the part of the impedance that is rolling off ( $a \neq 1$ ). For this reason, it is doubtful whether the Keil-Schnell or Krinsky-Wang criterion should apply to electron bunches. More about mode-coupling and will be given in the last section.

## 4.5 OBSERVATION AND CURE

In order for a bunch to be microwave unstable, the growth rate has to be much faster than the synchrotron frequency. For the Fermilab Main Ring, the synchrotron period was typically about 100 to 200 turns or 2 to 4 ms. A naive way to observe the microwave growth is to view the spectrum of the bunch over a large range of frequencies at a certain moment. However, the bunch spectrum produced by a network analyzer is usually via a series of frequency filters of narrow width, starting from low frequencies and working its way towards high frequencies. This process is time consuming. As soon as the filtering reaches the frequencies concerned, typically a few GHz, the microwave growth may have been stabilized already through bunch dilution, and therefore no growth signals will be recorded. The correct way is to set the network

analyzer at a narrow frequency span and look at the beam signal as a function of time. The frequency span is next set to an adjacent frequency interval and the observation repeated until the frequency range of a few GHz has been covered. Besides, we must make sure that the network analyzer is capable of covering the high frequency of a few GHz for the microwave growth signals. Also the cable from the beam detector to the network analyzer must be thick enough so that high-frequency attenuation is not a problem in signal propagation.

Since microwave instability occurs so fast, it is not possible to use a damper system to cure it. One way to prevent the instability is to blow up the bunch so that the energy spread is large enough to provide the amount of Landau damping needed. Another way is to reduce the impedance budget of the ring by smoothing out the beam pipe discontinuities. For negative-mass instability driven by the space-charge impedance just after transition, one can try to modify the ramp curve so that transition can be crossed faster. Of course, a  $\gamma_t$ -jump mechanism will be very helpful.

## EXERCISES

- 4.1. The dispersion relation of Eq. (4.18) can be rewritten in a simpler form. let us measure revolution angular frequency in terms of  $2S$ , the FWHM spread, which is related to the FWHM energy spread by

$$2S = -\eta\omega_0 \left. \frac{\Delta E}{E_0} \right|_{\text{FWHM}} . \quad (4.32)$$

We can then introduce a dimensionless reduced angular frequency  $x$  such that

$$n\omega - n\omega_0 = nxS \quad \text{and} \quad \Omega - n\omega_0 = nx_1S , \quad (4.33)$$

where we have used the fact the the collective angular frequency  $\Omega$  in Eq. (4.16) is close to  $n\omega_0$ . The frequency distribution function  $g_0(\omega)$  is now transformed to a distribution  $f(x)$  which is normalized to 1 when integrated over  $x$ . We have

$$\frac{dg_0(\omega)}{d\omega} d\omega = \frac{df(x)}{dx} \frac{dx}{d\omega} dx = \frac{1}{S} \frac{df(x)}{dx} dx . \quad (4.34)$$

- (a) Show that the dispersion relation (4.18) becomes

$$1 = -\frac{i2}{\pi}(U' + iV') \int \frac{f'(x)}{x_1 - x} dx , \quad (4.35)$$

where  $U'$  and  $V'$  are defined in Eq. (4.19).

- (b) When the beam current is just above threshold, the reduced collective angular frequency is written as  $x_1 = x_{1R} - i\epsilon$  where  $x_{1R}$  is real and  $\epsilon$  is an infinitesimal positive number. Show that the stability curve can be obtained from

$$1 = -\frac{i2}{\pi}(U' + iV') \left[ \wp \int \frac{f'(x)}{x_{1R} - x} dx + i\pi f'(x_{1R}) \right] . \quad (4.36)$$

by varying  $x_{1R}$ , where  $\wp$  denote the principal value of the of the integral.

- (c) show that the negative  $V'$ -intersect or the lowest point of the bell-shaped stability curve  $V'_{\text{in}}$  is given by

$$1 = -\frac{2V'_{\text{in}}}{\pi} \wp \int \frac{f'(x)}{x} dx . \quad (4.37)$$

Table I: Form factors in the Keil-Schnell criterion for various distributions.

Frequency Distribution		Form Factor		
$g_0(\omega)$	$f(x)$	$a$	$F$	Value
$\frac{3}{4\hat{\omega}} \left(1 - \frac{\omega^2}{\hat{\omega}^2}\right)$	$\frac{3}{4a} \left(1 - \frac{x^2}{a^2}\right)$	$a = \sqrt{2}$	$\frac{\pi a^2}{6}$	1.0472
$\frac{8}{3\pi\hat{\omega}} \left(1 - \frac{\omega^2}{\hat{\omega}^2}\right)^{3/2}$	$\frac{8}{3a} \left(1 - \frac{x^2}{a^2}\right)^{3/2}$	$a = \frac{1}{1 - 2^{-2/3}}$	$\frac{\pi a^2}{8}$	1.0613
$\frac{15}{16\hat{\omega}} \left(1 - \frac{\omega^2}{\hat{\omega}^2}\right)^2$	$\frac{15}{16a} \left(1 - \frac{x^2}{a^2}\right)^2$	$a = \frac{1}{1 - 2^{-1/2}}$	$\frac{\pi a^2}{10}$	1.0726
$\frac{315}{256\hat{\omega}} \left(1 - \frac{\omega^2}{\hat{\omega}^2}\right)^4$	$\frac{315}{256a} \left(1 - \frac{x^2}{a^2}\right)^4$	$a = \frac{1}{1 - 2^{-1/4}}$	$\frac{\pi a^2}{18}$	1.0970
$\frac{1}{\sqrt{2\pi}\sigma} \exp\left(-\frac{\omega^2}{2\sigma^2}\right)$	$\frac{1}{\sqrt{2\pi}a} \exp\left(-\frac{\omega^2}{2a^2}\right)$	$a = \frac{1}{\sqrt{2\ln 2}}$	$\frac{\pi a^2}{2}$	1.1331

In fact, the form factor in the Keil-Schnell criterion is given by  $F = |V'_{\text{in}}|$ .

(d) The form factor  $F$ 's in the Keil Schnell criterion for various frequency distribution functions are listed in Table I. Verify the results.

4.2. Using Eq. (4.36), plot the bell-shaped stability contours for the distributions listed in Table I as illustrated in Fig. 4.

4.3. Using Eq. (4.35), show that the constant-growth contours for the Gaussian distribution are given by

$$1 = \frac{i4\ln 2}{\pi}(U' + iV') [1 + i\sqrt{\pi\ln 2} x_1 w(\sqrt{\ln 2} x_1)], \quad (4.38)$$

where use has been made of the integral representation of the complex error function:

$$w(z) = \frac{i}{\pi} \int_{-\infty}^{\infty} \frac{e^{-t^2}}{z - t} dt. \quad (4.39)$$

Plot the contours in Fig. 3.

## 5 LONGITUDINAL COUPLED-BUNCH INSTABILITIES

When the wake does not decay within the bunch spacing, bunches talk to each other. Assuming  $M$  bunches of equal intensity equally spaced in the ring, there are  $\mu = 0, 1, \dots, M-1$  modes of oscillations in which the center-of-mass of a bunch *leads*<sup>†</sup> its predecessor by the phase  $2\pi\mu/M$ . In addition, an individual

<sup>†</sup>We can also formulate the problem by having the bunch *lags* its predecessor by the phase  $2\pi\mu'/M$  in the  $\mu'$ -th coupling mode. Then mode  $\mu'$  will be exactly the same as mode  $M-\mu$  discussed in the text.

bunch in the  $\mu$ -th coupled-bunch mode can oscillate in the synchrotron phase space about its center-of-mass in such a way that there are  $m = 1, 2, \dots$  azimuthal nodes in the perturbed longitudinal phase-space distribution. Of course, there will be in addition radial modes of oscillation in the perturbed distribution. The long-range wake can drive the coupled bunches to instability.

## 5.1 SACHERER INTEGRAL EQUATION

Because the beam particles execute synchrotron oscillations, it is more convenient to use circular coordinates  $r, \phi$  in the longitudinal phase space instead. We define

$$\begin{cases} x = r \cos \phi = \tau , \\ p_x = r \sin \phi = \frac{\eta}{\omega_s \beta^2} \frac{\Delta E}{E_0} , \end{cases} \quad (5.1)$$

so that the equations of motion become

$$\begin{cases} \frac{dx}{ds} = -\frac{\omega_s}{v} p_x , \\ \frac{dp_x}{ds} = \frac{\omega_s}{v} x - \frac{\eta}{E_0 \omega_s \beta^2} \langle F_0^{\parallel}(\tau; s) \rangle . \end{cases} \quad (5.2)$$

The phase-space distribution  $\psi$  of a bunch can be separated into the unperturbed or stationary part  $\psi_0$  and the perturbed part  $\psi_1$ :

$$\psi(\tau, \Delta E; s) = \psi_0(\tau, \Delta E) + \psi_1(\tau, \Delta E; s) . \quad (5.3)$$

The linearized Vlasov equation becomes

$$\frac{\partial \psi_1}{\partial s} - \frac{\omega_s}{v} p_x \frac{\partial \psi_1}{\partial x} + \frac{\omega_s}{v} x \frac{\partial \psi_1}{\partial p_x} - \frac{d\psi_0}{dp_x} \frac{\eta}{E_0 \omega_s \beta^2} \langle F_0^{\parallel}(\tau; s) \rangle = 0 . \quad (5.4)$$

Changing to the circular coordinates, the equation simplifies to

$$\frac{\partial \psi_1}{\partial s} + \frac{\omega_s}{v} \frac{\partial \psi_1}{\partial \phi} - \frac{\eta}{E_0 \omega_s \beta^2} \frac{d\psi_0}{dr} \sin \phi \langle F_0^{\parallel}(\tau; s) \rangle = 0 . \quad (5.5)$$

The perturbed distribution can be expanded azimuthally,

$$\psi_1(r, \phi; s) = \sum_m \alpha_m R_m(r) e^{im\phi - i\Omega s/v} , \quad (5.6)$$

where  $R_m(r)$  are functions corresponding to the  $m$ -th azimuthal,  $\alpha_m$  are the expansion coefficients, and  $\Omega/(2\pi)$  is the collective frequency to be determined. The Vlasov equation becomes

$$(\Omega - m\omega_s) \alpha_m R_m(r) e^{-i\Omega s/v} = \frac{iv\eta}{E_0 \omega_s \beta^2} \frac{d\psi_0}{dr} \int_{-\pi}^{\pi} \frac{d\phi}{2\pi} e^{-im\phi} \sin \phi \langle F_0^{\parallel}(\tau; s) \rangle . \quad (5.7)$$

Now consider the wake force acting on a beam particle at location  $s$  with time advance  $\tau$  relative to the synchronous particle due to all preceding particles passing through  $s$  at an earlier time. This force can be expressed as

$$\langle F_0^{\parallel}(\tau; s) \rangle = \frac{e^2}{C} \sum_{k=-\infty}^{\infty} \int_{-\infty}^{\infty} d\tau' \rho_1[\tau', s - kC - v(\tau' - \tau)] W_0'[kC + v(\tau' - \tau)] , \quad (5.8)$$

where only the perturbed density  $\rho_1$ , which is the projection of  $\psi_1$  onto the  $\tau$  axis, is included, because the unperturbed part should have been considered in the zeroth order of the Vlasov equation during the discussion of potential-well discussion. The summation over  $k$  takes care of the contribution of the wake left by the charge distribution in previous turns. The lower limit of the summation and the lower limit of the integral have been extended to  $-\infty$  because of the causality property of the wake function. Now there are  $M$  bunches and the synchronous particle in the  $\ell$ -th bunch is at location  $s_\ell$ . If the witness particle is in the  $n$ -th bunch,

$$\langle F_{0n}^{\parallel}(\tau; s) \rangle = \frac{e^2}{C} \sum_{k=-\infty}^{\infty} \sum_{\ell=0}^{M-1} \int_{-\infty}^{\infty} d\tau' \rho_\ell[\tau'; s - kC - (s_\ell - s_n) - v(\tau' - \tau)] W_0'[kC + (s_\ell - s_n) + v(\tau' - \tau)] . \quad (5.9)$$

We assume the bunches are identical and equally spaced. For the  $\mu$ -th coupled mode, we substitute in the above expression the perturbed density of the  $n$ -th bunch  $\rho_{1n}(\tau)e^{-i\Omega s/v}$  including the phase lead,

$$\rho_\ell(\tau; s) = \rho_{1n}(\tau)e^{i2\pi\mu(\ell-n)/M}e^{-i\Omega s/v} . \quad (5.10)$$

Now go to the frequency domain using the Fourier transforms

$$W_0'(v\tau) = \frac{1}{2\pi} \int_{-\infty}^{\infty} d\omega Z_0^{\parallel}(\omega)e^{-i\omega\tau} , \quad (5.11)$$

$$\rho_{1n}(\tau; s) = \int_{-\infty}^{\infty} d\omega \tilde{\rho}_{1n}(\omega)e^{i\omega\tau} . \quad (5.12)$$

In Eq. (5.9) above, we shall neglect<sup>‡</sup> the time delay  $\tau' - \tau$  because this will only amount to a phase delay  $\Omega(\tau' - \tau)$  where  $\Omega \approx m\omega_s$ , which is very much less than the phase change  $\omega_r(\tau' - \tau)$  during the bunch passage, where  $\omega_r/(2\pi)$  is the frequency of the driving resonant impedance. Substituting Eqs. (5.11) and (5.12) into Eq. (5.9) and integrating over  $\tau'$  and one of the  $\omega$ 's, the wake force for the  $\mu$ -th coupled-bunch mode becomes

$$\langle F_{0n\mu}^{\parallel}(\tau; s) \rangle = \frac{e^2}{C} \sum_{k=-\infty}^{\infty} \sum_{\ell=0}^{M-1} e^{i2\pi\mu(\ell-n)/M} e^{i\Omega(-s+kC+s_\ell-s_n)/v} \int_{-\infty}^{\infty} d\omega \tilde{\rho}_{1n}(\omega) Z_0^{\parallel}(\omega) e^{-i\omega(kC+s_\ell-s_n)/v} e^{i\omega\tau} . \quad (5.13)$$

Now the summation over  $k$  can be performed giving

$$\langle F_{0n\mu}^{\parallel}(\tau; s) \rangle = \frac{e^2}{C} \sum_{p=-\infty}^{\infty} \sum_{\ell=0}^{M-1} e^{i2\pi\mu(\ell-n)/M} e^{-i\Omega s/v + i\omega_p\tau} \omega_0 \tilde{\rho}_{1n}(\omega_p) Z_0^{\parallel}(\omega_p) e^{-ip\omega_0(s_\ell-s_n)/v} , \quad (5.14)$$

where  $\omega_p = p\omega_0 + \Omega$ . We next make use of the fact that the unperturbed bunches are equally spaced, or

$$s_\ell - s_n = \frac{\ell - n}{M} C . \quad (5.15)$$

Then the summation over  $\ell$  can be performed. The sum vanishes unless  $(p-\mu)/M = q$ , where  $q$  is an integer. The final result is

$$\langle F_{0n\mu}^{\parallel}(\tau; s) \rangle = \frac{e^2 M \omega_0}{C} e^{-i\Omega s/v} \sum_{q=-\infty}^{\infty} \tilde{\rho}_{1n}(\omega_q) Z_0^{\parallel}(\omega_q) e^{i\omega_q\tau} , \quad (5.16)$$

---

<sup>‡</sup> Without this approximation, only  $Z_0^{\parallel}$  will have the argument  $\omega_q$  in Eq. (5.16) below. The argument of  $\tilde{\rho}$  and the factor in front of  $\tau$  in the exponent will be replaced by  $\omega_q - \Omega$ .

where  $\omega_q = (qM + \mu)\omega_0 + \Omega$ .

Since the left side of the Vlasov equation is expressed in terms of the radial function  $R_m(r)$ , we want to do the same for the wake force. First, rewrite the perturbed density in the time domain,

$$\langle F_{0n\mu}^{\parallel}(\tau; s) \rangle = \frac{e^2 M \omega_0}{C} e^{-i\Omega s/v} \sum_{q=-\infty}^{\infty} Z_0^{\parallel}(\omega_q) \int d\tau' \rho_{1n}(\tau') e^{i\omega_q(\tau-\tau')} . \quad (5.17)$$

Since  $\rho_1(\tau')$  is the projection of the perturbed distribution onto the  $\tau'$  axis, we must have

$$\rho_{1n}(\tau') d\tau' = \int \psi_{1n}(\tau', \Delta E') d\tau' d\Delta E' \quad (5.18)$$

$$= \frac{E_0 \omega_s \beta^2}{\eta} \int \psi_{1n}(r', \phi') r' dr' d\phi' \quad (5.19)$$

$$= \frac{E_0 \omega_s \beta^2}{\eta} \sum_{m'} \alpha_{m'} \int R_{m'}(r') e^{im' \phi'} r' dr' d\phi' . \quad (5.20)$$

The wake force then takes the form

$$\langle F_{0n}^{\parallel}(\tau; s) \rangle = \frac{e^2 \omega_0 M}{2\pi C} \frac{E_0 \omega_s \beta^2}{\eta} e^{-i\Omega s/v} \sum_{q=-\infty}^{\infty} \sum_{m'} Z_0^{\parallel}(\omega_q) \int r' dr' d\phi' R_{m'}(r') e^{im' \phi'} e^{i\omega_q(\tau-\tau')} , \quad (5.21)$$

This wake force is next substituted into the Vlasov equation (5.7). The integrations over  $\phi$  and  $\phi'$  are performed in terms of Bessel function of order  $m$  using its integral definition

$$i^m J_m(z) = \frac{1}{2\pi} \int_{-\pi}^{\pi} d\phi e^{\pm i\phi + iz \cos \phi} , \quad (5.22)$$

the recurring relation

$$J_{m-1}(z) + J_{m+1}(z) = \frac{2m}{z} J_m(z) , \quad (5.23)$$

and the fact that

$$J_m(-z) = (-1)^m J_m(z) . \quad (5.24)$$

The result is the Sacherer integral equation for longitudinal instability for the  $m$ -th azimuthal  $\mu$ -th coupled-bunch mode,

$$(\Omega - m\omega_s) \alpha_m R_m(r) = -\frac{i2\pi e^2 M N \eta}{\beta^2 E_0 T_0^2 \omega_s} \frac{m}{r} \frac{dg_0}{dr} \sum_{m'} i^{m-m'} \alpha_{m'} \int r' dr' R_{m'}(r') \sum_q \frac{Z_0^{\parallel}(\omega_q)}{\omega_q} J_{m'}(\omega_q r') J_m(\omega_q r) , \quad (5.25)$$

where transformation of the unperturbed longitudinal distribution

$$\psi_0(r) d\tau d\delta E = \frac{\omega_s \beta^2 E_0}{\eta} \psi_0 dx dp_x = N g_0(r) r dr d\phi \quad (5.26)$$

has been made so that  $g_0$  is normalized to unity when integrated over  $r dr d\phi$ .

This is an eigen-function-eigen-value problem, the  $\alpha_m$ 's being the eigen-functions and  $\Omega$  the corresponding eigen-value. The solution is nontrivial. However, with some approximations, interesting results can be deduced. When the perturbation is not too strong so that the shift in frequency is much less than

the synchrotron frequency, there will not be coupling between different azimuthals. The integral equation simplifies to

$$(\Omega - m\omega_s)R_m(r) = -\frac{i2\pi e^2 MN\eta}{\beta^2 E_0 T_0^2 \omega_s} \frac{m}{r} \frac{dg_0}{dr} \int r' dr' R_m(r') \sum_q \frac{Z_0^{\parallel}(\omega_q)}{\omega_q} J_m(\omega_q r') J_m(\omega_q r) . \quad (5.27)$$

The spread in synchrotron frequency can be introduced by letting  $\omega_s$  be a function of  $r$ . Moving the factor  $\Omega - m\omega_s(r)$  to the right side, the radial distribution  $R_m$  can be eliminated by multiplying both sides by  $rJ_m(r)$  and integrating over  $dr$ . We then arrive at the dispersion relation,

$$1 = -\frac{i2\pi e^2 MNm\eta}{\beta^2 E_0 T_0^2 \omega_s} \sum_q \frac{Z_0^{\parallel}(\omega_q)}{\omega_q} \int dr \frac{dg_0}{dr} \frac{J_m^2(\omega_q r)}{\Omega - m\omega_s(r)} . \quad (5.28)$$

Stability and growth contours can be derived from the dispersion relation of Eq. (5.28) in just the same way as in the discussion of microwave instability for a single bunch.

When the spread in synchrotron frequency is small, Eq. (5.28) gives the frequency shift

$$\Omega - m\omega_s = \frac{i2\pi e^2 MNm\eta}{\beta^2 E_0 T_0^2 \omega_s} \sum_q \frac{Z_0^{\parallel}(\omega_q)}{\omega_q} \left[ -\int dr \frac{dg_0}{dr} J_m^2(\omega_q r) \right] , \quad (5.29)$$

where the expression inside the square brackets can be viewed as a distribution dependent form factor, which is positive definite because  $dg_0/dr$  is negative. Take the simple case of a single bunch of length  $2\hat{\tau}$  and uniform distribution in the longitudinal phase space. Then

$$g_0(r) = \frac{1}{\pi\hat{\tau}^2} \theta(\hat{\tau} - r) , \quad (5.30)$$

where  $\theta(x) = 1$  when  $x > 0$  and zero otherwise. The form factor becomes

$$F = \frac{1}{\pi\hat{\tau}^2} J_m^2(\omega_q \hat{\tau}) \approx \frac{\omega_q^2}{4\pi} \frac{1}{(m!)^2} \left( \frac{\omega_q \hat{\tau}}{2} \right)^{2m-2} , \quad (5.31)$$

where the assumption of a short bunch has been made in the last step. The growth rate driven by the impedance can now be written as

$$\frac{1}{\tau_m} = \frac{e^2 N \eta}{2\beta^2 E_0 T_0^2 \omega_s} \frac{m}{(m!)^2} \sum_q \left( \frac{\omega_q \hat{\tau}}{2} \right)^{2m-2} \omega_q \text{Re} Z_0^{\parallel}(\omega_q) , \quad (5.32)$$

where, for one bunch,  $\omega_q = q\omega_0 + \Omega$ .

The  $m=0$  mode is a trivial mode which gives  $\Omega_0 = 0$ . It describes the potential-well distortion mode addressed in Section 3 and is of not much interest here where the emphasis is on instabilities. The next azimuthal mode is  $m=1$  which describes dipole oscillations and we expect  $\Omega \approx \omega_s$ . Consider the situation of having the driving impedance as a resonance is so narrow that there is only one  $q > 0$  that satisfies

$$\omega_r \approx q\omega_0 \pm \omega_s , \quad (5.33)$$

where  $\omega_r/(2\pi)$  is the resonant frequency. The growth rate can therefore be expressed as

$$\frac{1}{\tau_1} = \text{Im} \Delta\omega_s = \frac{\eta e^2 N \omega_r}{2\beta^2 E_0 T_0^2 \omega_s} [\text{Re} Z_0^{\parallel}(q\omega_0 + \omega_s) - \text{Re} Z_0^{\parallel}(q\omega_0 - \omega_s)] , \quad (5.34)$$

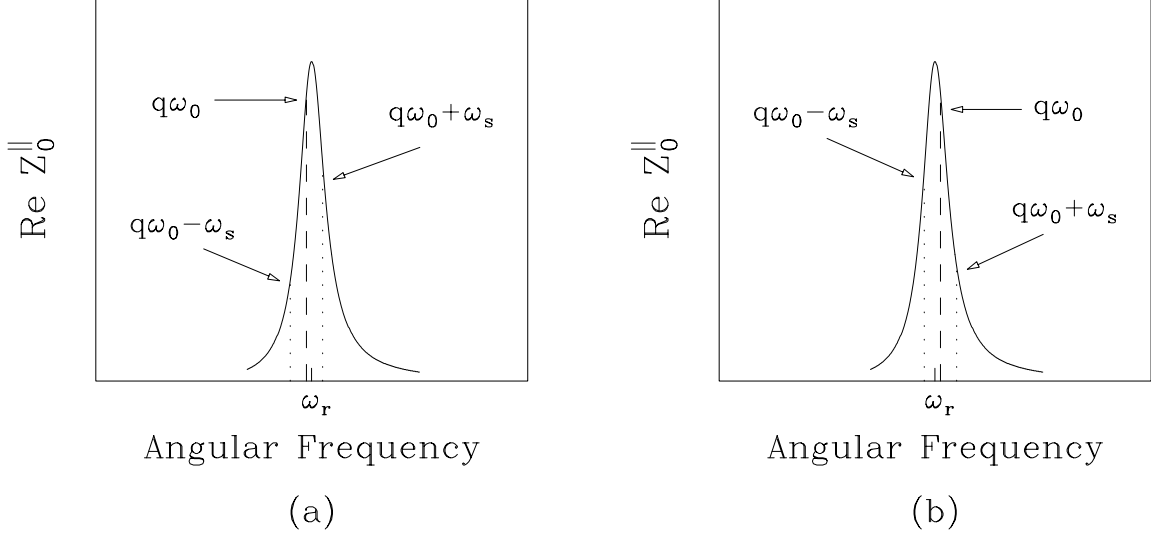


Figure 6: (a) Above transition, if the resonant frequency  $\omega_r$  is slightly above a revolution harmonic  $q\omega_0$ ,  $\mathcal{Re} Z_0^{\parallel}$  at the upper synchrotron side-band is larger than at the lower synchrotron side-band. The system is unstable. (b) Above transition, if  $\omega_r$  is slightly below a harmonic line,  $\mathcal{Re} Z_0^{\parallel}$  at the upper side-band is smaller than at the lower side-band, and the system is stable.

where the first term corresponds to positive frequency and the second negative frequency. If the resonant frequency is slightly above  $q\omega_0$  as illustrated in Fig. 6(a), we have  $\mathcal{Re} Z_0^{\parallel}(q\omega_0 + \omega_s) > \mathcal{Re} Z_0^{\parallel}(q\omega_0 - \omega_s)$ . Above transition, the growth rate will be positive or there is instability. On the other hand if  $\omega_r < q\omega_0$  as illustrated in Fig. 6(b), the growth rate is negative and the system is damped. This instability criterion was first analyzed by Robinson [13]. Note that the growth rate of Eq. (5.34) is independent of the bunch length when the bunch is short, implying that for the dipole mode, this is a point-bunch theory. More about Robinson stability criterion will be discussed in Section 5.3.

For  $M$  equal bunches, Eq. (5.34) becomes, for coupled-bunch mode  $\mu$ ,

$$\frac{1}{\tau_{1\mu}} = \frac{\eta e^2 N M \omega_r}{2\beta^2 E_0 T_0^2 \omega_s} [\mathcal{Re} Z_0^{\parallel}(qM\omega_0 + \mu\omega_0 + \omega_s) - \mathcal{Re} Z_0^{\parallel}(q'M\omega_0 - \mu\omega_0 - \omega_s)]. \quad (5.35)$$

When  $\mu = 0$ , both terms will contribute with  $q' = q$  and we have exactly the same Robinson's stability or instability as for the single bunch situation. This is illustrated in Fig. 7. When  $\mu = M/2$  if  $M$  is even, both terms will contribute with  $q' = q$ , and the same Robinson's stability or instability will apply. For the other  $M-2$  modes, only one term will be at or close to the resonant frequency and only one term will contribute. If the positive-frequency term contributes, we have instability. If the negative-frequency term contributes, we have damping instead. If one choose to speak in the language of only positive frequencies, there will be an upper and lower synchrotron side-band surrounding each revolution harmonic. Above transition, the coupled-bunch system will be unstable if the driving resonance leans towards the upper side-band and stable if it leans towards the lower side-band.

For the higher azimuthal modes ( $m > 1$ ) driven by a narrow resonance, we have the same Robinson

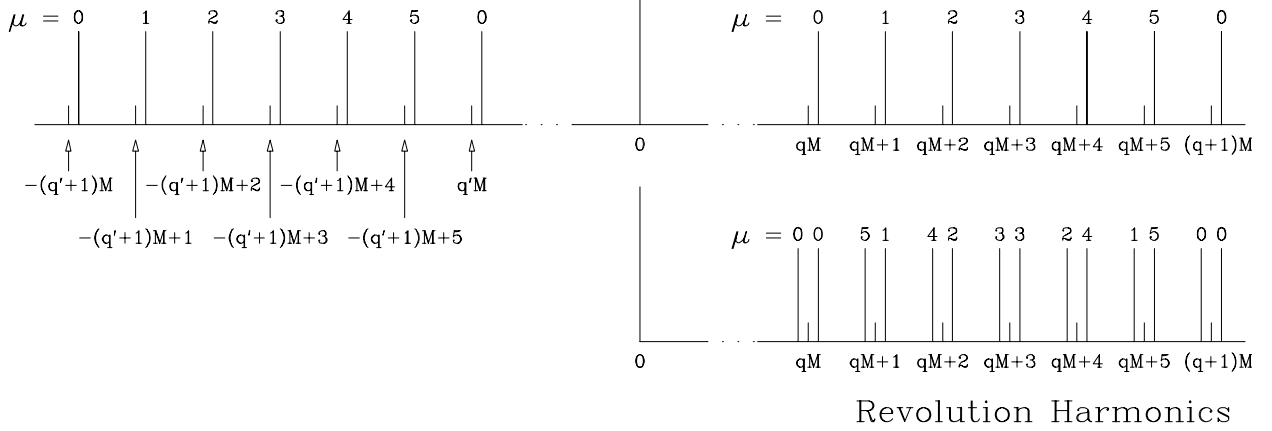


Figure 7: Top plot shows the synchrotron lines for both positive and negative revolution harmonics for the situation of  $M = 6$  identical equally-spaced bunches. The coupled-bunch modes  $\mu = 0, 1, 2, 3, 4, 5$  are listed at the top of the synchrotron lines. Lower plot shows the negative-harmonic side folded onto the positive-harmonic side. We see upper and lower side-band for each harmonic line.

instability. The growth rates are

$$\frac{1}{\tau_{m\mu}} = \frac{\eta e^2 N M \omega_r}{2\beta^2 E_0 T_0^2 \omega_s} \frac{m}{(m!)^2} \left( \frac{\omega_r \hat{\tau}}{2} \right)^{2m-2} [\text{Re } Z_0^{\parallel}(qM\omega_0 + \mu\omega_0 + \omega_s) - \text{Re } Z_0^{\parallel}(q'M\omega_0 - \mu\omega_0 - \omega_s)], \quad (5.36)$$

which depend on the bunch length as  $\hat{\tau}^{2m-2}$ . As a result, higher azimuthal instabilities for short bunches will be much more difficult to excite.

Landau damping can come from the spread of the synchrotron frequency. The spread due to the nonlinear sinusoidal rf wave form can be written as

$$\frac{\Delta\omega_s}{\omega_s} = \frac{2}{3} \left( \frac{1 + \sin^2 \phi_s}{1 - \sin^2 \phi_s} \right) \left( \frac{h\tau_L f_0}{2} \right)^2, \quad (5.37)$$

where  $\tau_L$  is the total length of the bunch and  $\phi_s$  is the synchronous angle. The mode will be stable if

$$\frac{1}{\tau} \lesssim \frac{\sqrt{m}}{4} \Delta\omega_s. \quad (5.38)$$

## 5.2 TIME DOMAIN

The longitudinal coupled-bunch instabilities can also be studied without going into the frequency domain. We are employing the same Vlasov equation in Eq. (5.7), but using the wake function of a resonance in the time domain [14].

The wake function for a resonance with resonant frequency  $\omega_r/(2\pi)$ , shunt impedance  $R_s$  and quality factor  $Q$  was given in Eq. (1.22). For a narrow resonance with  $\alpha = \omega_r/(2Q) \ll \omega_r$ , we can neglect the sine term<sup>§</sup> and simplify the wake function to

$$W'_0(z) = \frac{\omega_r R_s}{Q} e^{-\alpha z/v} \cos \frac{\omega_r z}{v} \quad \text{when } z > 0. \quad (5.39)$$

<sup>§</sup>The sine term can be included at the expense of a slightly more complicated derivation.

The wake force is then given by

$$\langle F_0^{\parallel}(\tau; s) \rangle = \frac{e^2 \omega_r R_s}{QC} \int_{\tau}^{\infty} d\tau' e^{-\alpha(\tau'-\tau)} \cos[\omega_r(\tau'-\tau)] \rho[\tau'; s - v(\tau'-\tau)] . \quad (5.40)$$

Now let  $\rho(\tau; s)$  represent the line density of the individual bunch, which has a phase lead of  $2\pi\mu/M$  for mode  $\mu$  compared with the preceding bunch  $\tau_{\text{sep}} = T_0/M$  ahead, and is influenced by all the preceding bunches. The location argument  $s$  of  $\rho$  in Eq. (5.40) becomes<sup>¶</sup>  $s - k\tau_{\text{sep}} - v(\tau'-\tau)$ , with  $k = 0, 1, 2, \dots$ . For simplicity, we neglect the time delay  $\tau'-\tau$ . In the time variation  $e^{-i\Omega s/v}$  where  $\Omega \approx m\omega_s$ , this delay causes a phase delay  $\Omega(\tau'-\tau)$  which is negligible in comparison with the phase change due to the resonator. We will also neglect the variation in the attenuation factor over one bunch in  $e^{-\alpha(\tau'-\tau)}$ . Then the wake force exerted on a particle in the  $\mu$ -th coupled-bunch mode can be written as

$$\langle F_{0\mu}^{\parallel}(\tau; s) \rangle = \frac{e^2 \omega_r R_s}{QC} \sum_{k=0}^{\infty} e^{2\pi i k \mu / M - k \alpha \tau_{\text{sep}}} \int_{\text{one bunch}} d\tau' \cos[\omega_r(\tau'-\tau) + k\tau_{\text{sep}}] \rho_1(\tau') e^{-i\Omega(s/v - k\tau_{\text{sep}})} . \quad (5.41)$$

It is worth pointing out that the lower limits of the summation and integration *cannot* be extended to  $-\infty$  as before, because the explicit expression of the wake function has been used. Note that only the perturbed line density  $\rho_1$  is included. This is because the unperturbed part  $\rho_0$  should have been taken care of in the potential-well distortion consideration. Changing the integration variables from  $(\tau, \Delta E)$  to  $(r, \phi)$  while keeping only the azimuthal  $m$ ,

$$\rho_1(\tau') d\tau' = \alpha_m R_m(r') e^{im\phi'} d\tau' d\Delta E' = \frac{E_0 \omega_s \beta^2}{\eta} \alpha_m R_m(r') e^{im\phi'} r' dr' d\phi' . \quad (5.42)$$

Substituting the wake force into Eq. (5.7), we arrive at

$$\begin{aligned} (\Omega - m\omega_s) R_m(r) &= \frac{ie^2 N \eta \omega_r R_s}{2\pi \beta^2 E_0 Q T_0 \omega_s} \frac{dg_0}{dr} \sum_{k=0}^{\infty} e^{2\pi i k \mu / M - k(\alpha - i\Omega)\tau_{\text{sep}}} \times \\ &\times \int_0^{\infty} r' dr' R_m(r') \int_{-\pi}^{\pi} d\phi e^{-im\phi} \sin \phi \int_{-\pi}^{\pi} d\phi' e^{im\phi'} \cos[\omega_r(r' \cos \phi' - r \cos \phi) + k\tau_{\text{sep}}] , \end{aligned} \quad (5.43)$$

where again we have used the unperturbed distribution  $g_0(r)$  given by Eq.(5.26) which is normalized to unity. The result is

$$\begin{aligned} (\Omega - m\omega_s) R_m(r) &= -\frac{2\pi e^2 N R_s m \eta}{\beta^2 E_0 Q T_0 \omega_s} \frac{dg_0}{dr} \times \\ &\times \sum_{k=0}^{\infty} e^{2\pi i k \mu / M - k(\alpha - i\Omega)\tau_{\text{sep}}} \sin(k\omega_r \tau_{\text{sep}}) \int_0^{\infty} dr' R_m(r') \frac{r' J_m(\omega_r r') J_m(\omega_r r)}{r} . \end{aligned} \quad (5.44)$$

Finally, we introduce Landau damping by allowing the synchrotron frequency to be a function of the radial distance from the center of the bunch in the longitudinal phase phase. Moving  $\Omega - m\omega_s(r)$  to the right side and performing an integration over  $r dr$ , we can eliminate  $R_m$  and obtain the dispersion relation

$$1 = -i \frac{2\pi e^2 N R_s m M \eta}{\beta^2 E_0 \omega_s \omega_r T_0^2} D(\alpha \tau_{\text{sep}}) \int_0^{\infty} dr \frac{dg_0}{dr} \frac{J_m^2(\omega_r r)}{\Omega - m\omega_s(r)} , \quad (5.45)$$

where we have defined the function<sup>||</sup>

$$D(\alpha \tau_{\text{sep}}) = -i 2\alpha \tau_{\text{sep}} \sum_{k=0}^{\infty} e^{2\pi i k \mu / M - k(\alpha - i\Omega)\tau_{\text{sep}}} \sin k\omega_r \tau_{\text{sep}} , \quad (5.46)$$

<sup>¶</sup> Here we include the term  $k\tau_{\text{sep}}$  which Sacherer had left out. This term is important to exhibit Robinson's criterion of phase stability.

<sup>||</sup> We would like  $D = \pm 1$  when the resonance is at the upper/lower side-band. As a result, our definition of  $D$  differs from Sacherer's by a phase.

which contains all the information about the quality factor of the resonance and its location with respect to the revolution harmonics. It is interesting to note that Eq. (5.45) closely resembles Eq. (5.28). It will be shown below that  $D = 1$  for a narrow resonance with the resonant peak located at  $(qM + \mu)\omega_0 + m\omega_s$ . Thus the two dispersion relations are identical. In fact, they are the same even when the resonant peak is not exactly located at a synchrotron line.

Now let us study the function  $D(\alpha\tau_{\text{sep}})$ . Noting that the bunch separation is  $\tau_{\text{sep}} = T_0/M$ , this function can be rewritten as

$$D(\alpha\tau_{\text{sep}}) = \alpha\tau_{\text{sep}} \left( \frac{1}{1-e^{x_+}} - \frac{1}{1-e^{x_-}} \right), \quad (5.47)$$

where

$$x_{\pm} = \frac{2\pi i}{M} \left( q_{\pm}M + \mu + m \frac{\omega_s}{\omega_0} \mp \frac{\omega_r}{\omega_0} \right) - \alpha\tau_{\text{sep}}. \quad (5.48)$$

The  $q_{\pm}M$  term comes about because we can replace  $\mu$  in Eq. (5.46) by  $q_{\pm}M + \mu$ , where  $q_{\pm}$  are positive/negative integers and  $\mu = 0, 1, \dots, M-1$ . When the resonance is extremely narrow, we have  $\alpha\tau_{\text{sep}} = \omega_r\tau_{\text{sep}}/(2Q) \ll 1$ . The two terms in Eq. (5.47) almost cancel each other so that  $D(\alpha\tau_{\text{sep}}) \approx 0$  unless  $\omega_r \approx (|q_{\pm}|M \pm \mu)\omega_0$ . For modes  $\mu \neq 0$  and  $\mu \neq \frac{1}{2}M$  if  $M$  is even, only one of the two terms in Eq. (5.47) contributes. If  $\omega_r \approx (|q_{\pm}| \pm \mu)\omega_0 \pm m\omega_s$ , we have  $|x_+| \ll 1$  or  $|x_-| \ll 1$  and

$$D(\alpha\tau_{\text{sep}}) \approx \mp \frac{\alpha\tau_{\text{sep}}}{x_{\pm}} = \frac{-i\omega_r/(2Q)}{\omega_r - [(|q_{\pm}|M \pm \mu)\omega_0 \pm m\omega_s] \mp i\omega_r/(2Q)} \approx \pm 1. \quad (5.49)$$

When  $\mu = 0$  or  $\mu = M/2$  if  $M$  is even, it is possible to choose  $q_+$  and  $q_-$  so that both terms will contribute. We have

$$D \approx \frac{-i\omega_r/(2Q)}{\omega_r - [(q_+M + \mu)\omega_0 + m\omega_s] - i\omega_r/(2Q)} + \frac{-i\omega_r/(2Q)}{\omega_r - [(|q_-|M - \mu)\omega_0 - m\omega_s] + i\omega_r/(2Q)}, \quad (5.50)$$

where  $q_+ = |q_-|$  for  $\mu = 0$  and  $|q_-| = q_+ + 1$  for  $\mu = M/2$ . Note that Eq. (5.50) is just proportional to  $[Z_0^{\parallel}(q_+M\omega_0 + \mu\omega_0 + m\omega_s + i\alpha) - Z_0^{\parallel}(|q_-|M\omega_0 - \mu\omega_0 - m\omega_s - i\alpha)]$ , and we recover the Robinson's stability criterion derived in Eq. (5.35).

On the other hand, when the resonance is broad,  $\alpha\tau_{\text{sep}} \gg 1$ . The  $k = 1$  in Eq. (5.46) dominates since  $k = 0$  does not contribute and we have instead

$$D(\alpha\tau_{\text{sep}}) \approx -i2\alpha\tau_{\text{sep}} \sin(\omega_r\tau_{\text{sep}}) e^{2\pi i\mu/M - \alpha\tau_{\text{sep}}}. \quad (5.51)$$

Therefore coupled-bunch modes near  $\mu = \pm \frac{1}{4}M$  are most strongly excited, although  $|D|$  will be much less than unity. Figure 8 plots  $|D|$  versus  $\omega_r/\omega_0$  for the situation of  $M = 10$  bunches. The solid lines show  $|D| \approx 1$  for narrow resonance. The dotted curve are for broad-band resonance when the bunch to bunch attenuation decrement is  $\alpha\tau_{\text{sep}} = 4$ ; the values of  $|D|$  are small and appear to be mode-independent. The dashed curves correspond the intermediate case with bunch-to-bunch attenuation decrement  $\alpha\tau_{\text{sep}} = 1$ . From left to right, they are for modes  $\mu = 0, 1$  and  $9, 2$  and  $8, 3$  and  $7, 4$  and  $6, 5$ . We see that  $|D|_{\text{max}}$  is roughly the same for each mode. Note that  $\alpha\tau_{\text{sep}} = 1$  translates into  $(\Delta\omega_r/\omega_0)_{\text{FWHM}} = M/\pi = 3.2$  or the resonance covers more than 3 revolutionary harmonics. It is demonstrated in the figure that all modes will not be excited if the  $\omega_r/\omega_0$  falls exactly on  $qM$  or  $q(\frac{1}{2}M)$  if  $M$  is even. This is because in drawing the plot, the limit  $\omega_s \rightarrow 0$  has been taken. Figures 9 plots  $|D|_{\text{max}}$  versus the bunch-to-bunch decrement  $\alpha\tau_{\text{sep}}$ , showing that it is less than 5% from unity when  $\alpha\tau_{\text{sep}} < 0.55$ .

In the event that the spread in synchrotron frequency is small, we can obtain from Eq. (5.45) the

Solid: no decay between bunches  
Dashes: decay between bunches  $e^{-1}$   
Dots: decay between bunches  $e^{-4}$

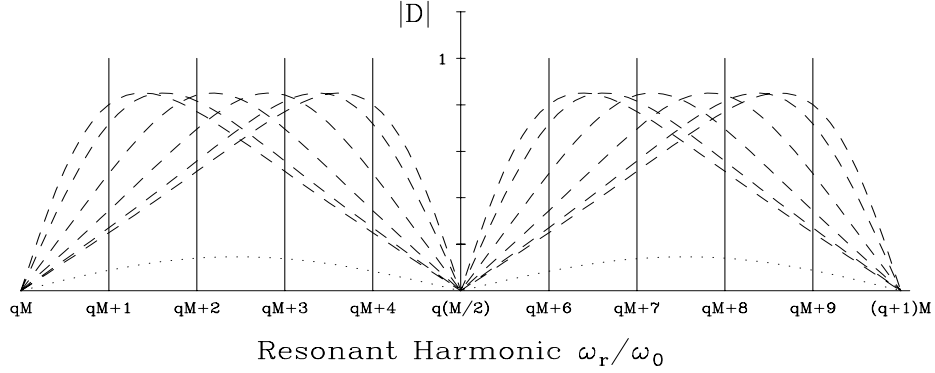


Figure 8:  $|D|$  as functions of resonant harmonic  $\omega_r/\omega_0$  for  $M = 10$  bunches when bunch-to-bunch decay decrement  $\alpha\tau_{\text{sep}} \ll 1$  for narrow-band resonance (solid),  $\alpha\tau_{\text{sep}} = 4$  for broad-band resonance (dots), and  $\alpha\tau_{\text{sep}} = 1$  for resonance in between (dashes). The dashed curves from left to right represent coupled-bunch modes  $\mu = 0, 1$  and  $9, 2$  and  $8, 3$  and  $7, 4$  and  $6, 5$ . The excitations at  $\omega_r/\omega_0 = 0$ , or  $M/2$  is always zero, because we have set the synchrotron frequency to zero in the plot.

synchrotron frequency shift

$$\Omega - m\omega_s = -\frac{i2\pi e^2 N R_s m M \eta}{\beta^2 E_0 \omega_s \omega_r T_0^2} D(\alpha\tau_{\text{sep}}) \int_0^\infty dr \frac{dg_0}{dr} J_m^2(\omega_r r), \quad (5.52)$$

where the integral can be viewed as a form factor which is distribution dependent. A form factor

$$F_m(\Delta\phi) = -\frac{4\pi m \hat{\tau}}{\omega_r} \int_0^\infty dr \frac{dg_0}{dr} J_m^2(\omega_r r) \quad (5.53)$$

can now be defined for each azimuthal, where  $\hat{\tau}$  is the half bunch length and  $\Delta\phi = 2\omega_r \hat{\tau}$  is the change in phase of the resonator during the passage of the whole bunch. Then the frequency shift can be rewritten as

$$\Omega - m\omega_s = \frac{i\eta e^2 N M R_s}{4\pi\beta^2 E_0 \nu_s T_0 \hat{\tau}} D(\alpha\tau_0) F_m(\Delta\phi), \quad (5.54)$$

where  $\nu_s = \omega_s/\omega_0$  is the synchrotron tune.

We take as an example the parabolic distribution in the longitudinal phase space,\*\* which implies

$$g_0(r) = \frac{2}{\pi\hat{\tau}^4}(\hat{\tau}^2 - r^2) \quad \text{and} \quad \frac{dg_0}{dr} = -\frac{4r}{\pi\hat{\tau}^4}. \quad (5.55)$$

The form factor is

$$\begin{aligned} F_m(\Delta\phi) &= \frac{32m}{\Delta\phi} \int_0^1 J_m^2\left(\frac{1}{2}\Delta\phi x\right) x dx \\ &= \frac{16m}{\Delta\phi} \left[ J_m^2\left(\frac{1}{2}\Delta\phi\right) - J_{m+1}\left(\frac{1}{2}\Delta\phi\right) J_{m-1}\left(\frac{1}{2}\Delta\phi\right) \right], \end{aligned} \quad (5.56)$$

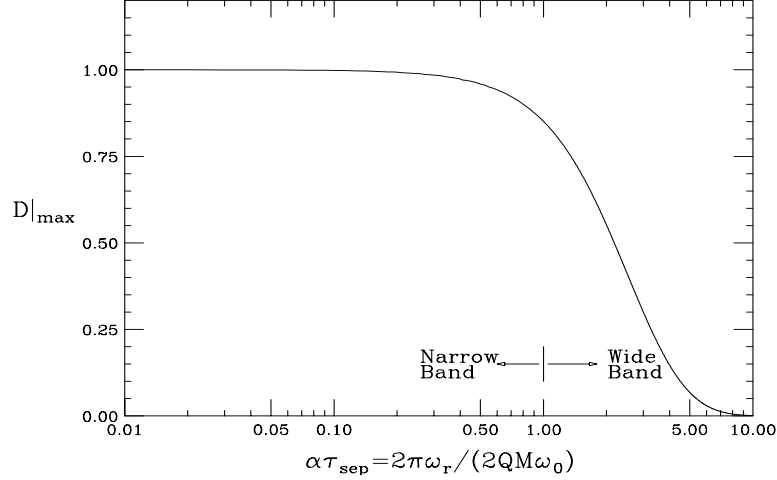


Figure 9:  $|D|_{\max}$  as a function of bunch-to-bunch decay decrement  $\alpha\tau_{\text{sep}}$ . Note that  $|D|_{\max} \approx 1$  for narrow resonances but drops very rapidly as the resonance becomes broader.

which is plotted in Fig. 10 for  $m = 1$  to 6. The form factor specifies the efficiency with which the resonator can drive a given mode. We see that the maximum value of  $F_1$  for the dipole mode occurs when  $\Delta\phi \approx \pi$ . This is to be expected because the head and tail of the bunch will be driven in opposite directions. Similarly, the quadrupole or breathing mode is most efficiently driven when  $\Delta\phi \approx 2\pi$ , and so on for the higher modes. In general, mode  $m$  is most efficiently driven when the resonator frequency is  $\Delta\phi \approx m\pi$ . Note also that the maximum value of  $F_m$  drops faster than  $m^{-1/2}$ , implying that higher azimuthal modes are harder to excite.

For small  $\Delta\phi$ ,  $F_1 \approx \frac{1}{2}\Delta\phi$ . From Eq. (5.52), the growth rate for the dipole mode above transition can be written as

$$\frac{\eta e^2 N M R_s \omega_r}{2\beta^2 E_0 \omega_s T_0^2}, \quad (5.57)$$

which agrees with the expression in Eq. (5.35) derived for small bunches.

### 5.3 RF DETUNING AND ROBINSON'S STABILITY CRITERIA

The rf cavity has a loaded shunt impedance  $R_s$ , a loaded quality factor  $Q_L$ , and resonates at frequency  $\omega_r/(2\pi)$ . Corresponding to a beam particle revolving with frequency  $\omega_0/(2\pi)$ , the rf frequency is  $\omega_{\text{rf}}/(2\pi) = h\omega_0/(2\pi)$ , where  $h$  is the rf harmonic. The impedance of the cavity seen by the particle at  $\omega_{\text{rf}}/(2\pi)$  can be written approximately as

$$Z_{\text{cav}} = \frac{R_s}{1 - jQ_L \left( \frac{\omega_r}{\omega_{\text{rf}}} - \frac{\omega_{\text{rf}}}{\omega_r} \right)} \approx R_s \cos \psi e^{j\psi}, \quad (5.58)$$

where  $\psi$  is the rf detuning angle, which is defined as

$$\tan \psi = 2 Q_L \frac{\omega_r - \omega_{\text{rf}}}{\omega_r}. \quad (5.59)$$

Note that in this section we have used  $j$  instead of  $-i$ , because phasor diagrams are customarily drawn using this convention. The detuning, which implies  $\psi \neq 0$ , is necessary because (1) we want the load to appear

---

\*\*This is different from the so-called parabolic distribution, which is actually parabolic line density.

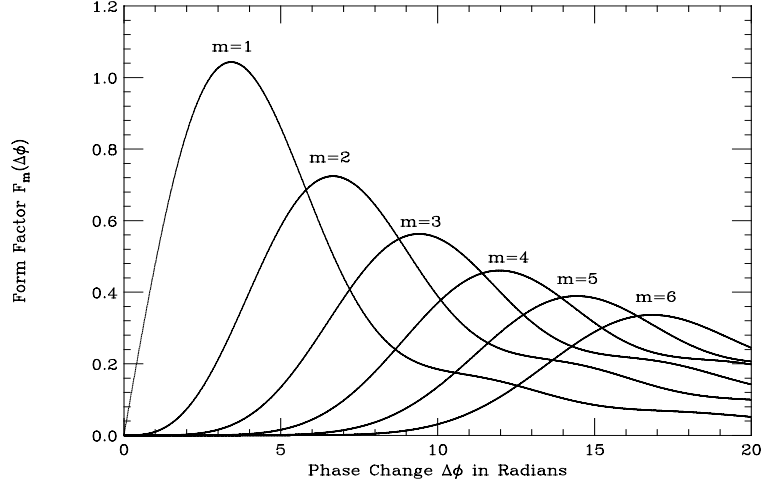


Figure 10: Form factor for longitudinal oscillation inside a bunch with  $m = 1, 2, 3, 4, 5$  and 6 nodes. The unperturbed parabolic distribution in the longitudinal phase space is assumed.

real to the generator (the generator current  $i_g$  in phase with the cavity gap voltage  $V_{rf}$ ) so that there will not be any power reflection to the generator, and (2) both the generator voltage  $V_g$  and the beam-loading voltage  $V_{im}$  contribute to the cavity gap voltage. This is illustrated in the phasor diagram in Fig. 11, where the tilde represents a phasor rotating counter-clockwise with angular frequency  $\omega_{rf}$ . Here, we assume most of the transient beam-loading has been cancelled; therefore, the image current phasor  $\tilde{i}_{im}$  has a magnitude much smaller than that of the beam current phasor  $\tilde{i}_b$ . According to Eq. (5.58), we see from Fig. 11 that both the beam-loading voltage phasor  $\tilde{V}_{im}$  and the generator voltage phasor  $\tilde{V}_g$  are at a phase  $\psi$  ahead of their respective current phasors  $\tilde{i}_{im}$  and  $\tilde{i}_g$ . Since these two voltage phasors add up to give the gap voltage phasor  $\tilde{V}_{rf}$  which has a synchronous angle  $\phi_s$ , we must have after dividing by  $R_s \cos \phi$ ,

$$i_g \sin \psi = i_{im} \sin\left(\frac{\pi}{2} - \phi_s + \psi\right). \quad (5.60)$$

Resolving the current contributions along  $\tilde{i}_g$ , we have

$$i_g = i_0 + i_{im} \sin \phi_s, \quad (5.61)$$

where  $i_0 = V_{rf}/R_s$  is the total current in phase with the cavity gap voltage. Eliminating  $i_g$ , we arrive at

$$\tan \psi = \frac{i_{im} \cos \phi_s}{i_0}. \quad (5.62)$$

Now let us study the conditions for phase stability. Suppose that the beam particle has a slightly larger energy than the synchronous particle. After a revolution or  $h$  rf periods,  $\tilde{i}_b$  in Fig. 11 will be ahead of the  $x$ -axis by a small angle  $\epsilon > 0$  if it is below transition. Then the accelerating voltage it sees will be  $V_{rf} \sin(\phi_s - \epsilon)$  instead of  $V_{rf} \sin \phi_s$ , or an extra decelerating voltage of  $\epsilon V_{rf} \cos \phi_s$ , and it receives less energy from the cavity than the synchronous particle. The motion is therefore stable. Therefore to establish stable phase oscillation when beam loading can be neglected, one requires

$$\begin{cases} 0 < \phi_s < \frac{\pi}{2} & \text{below transition,} \\ \frac{\pi}{2} < \phi_s < \pi & \text{above transition.} \end{cases} \quad (5.63)$$

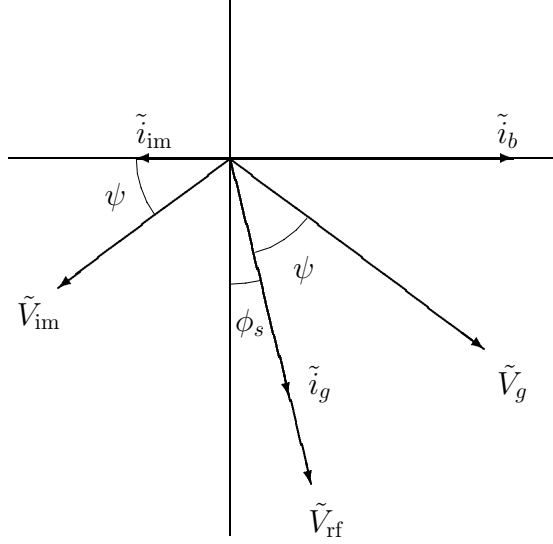


Figure 11: Phasor plot showing the vector addition of the generator voltage phasor  $\tilde{V}_g$  and the beam-loading voltage phasor  $\tilde{V}_{im}$  to give the gap voltage phasor  $\tilde{V}_{rf}$  in a rf cavity. Note the detuning angle  $\psi$  which put the gap current phasor  $\tilde{i}_g$  in phase with the gap voltage phasor.

From Eqs. (5.59) and (5.62), this translates into

$$\begin{cases} \tan \psi > 0 & \text{or } \omega_r > \omega_{rf} & \text{below transition,} \\ \tan \psi < 0 & \text{or } \omega_r < \omega_{rf} & \text{above transition,} \end{cases} \quad (5.64)$$

which is just Robinson's criterion [13] for phase stability discussed in the previous subsection.

When beam loading is included, the gap voltage phasor  $\tilde{V}_{rf}$  will be modified also, because the image current phasor  $\tilde{i}_{im}$  and hence the beam-loading voltage phasor  $\tilde{V}_{im}$  also advance by the small angle  $\epsilon$  after  $h$  rf periods. The extra beam-loading voltage phasor is  $\epsilon i_{im} R_s \cos \psi e^{j(\psi+3\pi/2)}$ . If  $\psi < 0$ , this phasor will point into the 3rd quadrant and decelerate the particle in concert with  $\epsilon V_{rf} \cos \phi_s$ , causing no instability. On the other hand, if  $\psi > 0$ , this phasor will point into the 4th quadrant and accelerate the particle instead. To be stable, the extra accelerating voltage on the beam must be less than the amount of decelerating voltage  $\epsilon V_{rf} \cos \phi_s$ , or

$$\frac{i_{im}}{i_0} < \frac{\cos \phi_s}{\sin \psi \cos \psi} \quad \begin{cases} \psi > 0 & \text{below transition,} \\ \psi < 0 & \text{above transition,} \end{cases} \quad (5.65)$$

which is called Robinson's *high-intensity criterion* for phase stability. Satisfying this criterion just enables stable oscillating like sitting inside a stable potential well and there will not be any damping. Violating this criterion will place the particle in an unstable potential well so that phase oscillation will not be possible.

## EXERCISES

- 5.1. Above/below transition with the resonant frequency offset by  $\Delta\omega = \pm(\omega_r - h\omega_0)$ , the bunch suffers Robinson's instability. Assuming that both  $\omega_s$  and  $|\Delta\omega|$  are much less than the resonator width

$\omega_r/(2Q)$  which, in turn, is much less than  $\omega_0$ , and using the expression for resonant impedance in Eq. (1.16), show that the Robinson growth rate in Eq. (5.34) can be written as

$$\frac{1}{\tau} = \frac{4e^2 N R_s Q^2 \eta \Delta\omega}{\pi \beta^2 E_0 h T_0} . \quad (5.66)$$

Robinson's instability is usually more pronounced in electron than proton machines because high shunt impedance and quality factor are often used in the rf system. Take for example a ring of circumference 180 m with slip factor  $|\eta| = 0.03$ . To store a typical bunch with  $1 \times 10^{11}$  electrons at  $E_0 = 1$  GeV, one may need a rf system with  $h = 240$ ,  $R_s = 1.0$  M $\Omega$ , and  $Q = 2000$ . On the other hand, to store a bunch of  $1 \times 10^{11}$  protons at  $E_0 = 1$  GeV in the same ring, one may need a rf system with  $h = 4$ ,  $R_s = 0.12$  M $\Omega$ , and  $Q = 45$ . Compare the Robinson growth rates for the two situations when the resonant frequencies are offset in the wrong directions by  $|\Delta\omega| = \omega_s$ . Assume the synchrotron tune to be 0.01 in both cases.

- 5.2. In Section 5.3, rf-detuning and Robinson's stability condition have been worked out below transition. Show that above transition the detuning according the Fig. 11 leads to instability. Draw a new phasor diagram for the situation above transition with stable rf-detuning. Rederive Robinson's high-intensity stability criterion above transition.
- 5.3. Derive all the expressions in the Section 5.2 on Sacherer's approach to coupled-bunch growth rate driven by a resonance.
- 5.4. Using the definition of the form factor in Eq. (5.53), compute numerically the form factor when the unperturbed distribution is bi-Gaussian. The half bunch length can be taken as  $\hat{\tau} = \sqrt{6}\sigma_\tau$ , where  $\sigma_\tau$  is the rms bunch length.

## 6 TRANSVERSE INSTABILITIES

Consider a coasting beam of current  $I_0$ . A particle inside oscillates with betatron tune  $\nu_\beta$ . The equation of motion for the vertical coordinate  $y$  is, according to Eq. (1.6)

$$\frac{d^2 y}{ds^2} + \frac{\omega_\beta^2}{v^2} y = \frac{\langle F_1^\perp \rangle}{\beta^2 E_0} = \frac{ieI_0 Z_1^\perp}{\beta E_0 C} y . \quad (6.1)$$

This causes an angular frequency shift of the betatron oscillation

$$\Delta\omega_\beta = -\frac{ie\beta c^2}{2\omega_\beta E_0} \frac{Z_1^\perp I_0}{C} , \quad (6.2)$$

the imaginary part of which, if positive, is the growth rate. The frequency at which the impedance is evaluated is  $\omega_p = p\omega_0 + \omega_\beta$ ,  $p$  being an integer, because the coasting beam contributes  $p\omega_0$  and the transverse motion  $\omega_\beta$ . The reactive part of  $Z_1^\perp(\omega)$  produces a real frequency shift. Since  $\mathcal{Re} Z_1^\perp(\omega) \geq 0$  when  $\omega \geq 0$ , the resistive part causes instability for negative frequency. Therefore only coasting-beam modes with  $p < -\nu_\beta$  can be unstable, where  $\nu_\beta = \omega_\beta/\omega_0$  is the betatron tune.

### 6.1 SACHERER INTEGRAL EQUATION

For bunched beam, longitudinal motion has to be included. Just as for synchrotron oscillations, it is more convenient to change from  $(y, p_y)$  to the circular coordinates  $(r_\beta, \theta)$  in the transverse betatron phase

space. Following Eq. (5.1), we have

$$\begin{cases} y = r_\beta \cos \theta \\ p_y = r_\beta \sin \theta , \end{cases} \quad (6.3)$$

and Eq. (6.1) is transformed into

$$\begin{cases} \frac{dy}{ds} = -\frac{\omega_\beta}{v} p_y \\ \frac{dp_y}{ds} = \frac{\omega_\beta}{v} y - \frac{c}{E_0 \omega_\beta \beta} \langle F_1^\perp(\tau; s) \rangle . \end{cases} \quad (6.4)$$

The Hamiltonian for motions in both the longitudinal phase space and transverse phase space can be written as

$$H = H_\parallel + H_\perp , \quad (6.5)$$

where  $H_\parallel$  is the same Hamiltonian given by Eq. (2.7) describing longitudinal motion while  $H_\perp$  is the additional term coming from the equations of motion in the transverse phase space as given by Eq. (6.4). We note that the transverse force  $\langle F_1^\perp(\tau; s) \rangle$  in Eq. (6.4) depends on the longitudinal variable  $\tau$ ; therefore

$$[H_\parallel, H_\perp] \neq 0 . \quad (6.6)$$

We assume that the perturbation is small and synchro-betatron coupling is avoided. Then

$$[H_\parallel, H_\perp] \approx 0 . \quad (6.7)$$

This implies that in the transverse phase space, the azimuthal modes  $m_\perp = 1, 2, \dots$ , and the radial modes  $k_\perp = 1, 2, \dots$  are good eigen-modes. In fact, this is very reasonable because at small perturbation, the transverse azimuthal modes  $m_\perp$  correspond to frequencies  $m_\perp \omega_\beta$  with separation  $\omega_\beta$ . Since

$$\omega_\beta \gg \omega_0 \gg \omega_s , \quad (6.8)$$

the possibility for different transverse azimuthals to couple is remote. A direct result of Eq. (6.7) is the factorization of the bunch distribution  $\Psi$  in the combined longitudinal-transverse phase space; i.e.,

$$\Psi(r, \phi; r_\beta, \theta) = \psi(r, \phi) f(r_\beta, \theta) , \quad (6.9)$$

where  $\psi(r, \phi)$  is the distribution in the longitudinal phase space and  $f(r_\beta, \theta)$  the distribution in the transverse phase space. Now decomposed  $\psi$  and  $f$  into the unperturbed parts and the perturbed parts:

$$\begin{aligned} \psi(r, \phi) &= \psi_0(r) + \psi_1(r, \phi) , \\ f(r_\beta, \theta) &= f_0(r_\beta) + f_1(r_\beta, \theta) . \end{aligned} \quad (6.10)$$

When substituted into Eq. (6.9), there are four terms. The term  $\psi_1 f_0$  implies only the longitudinal-mode excitations driven by the longitudinal impedance without any transverse excitations. This is what we have discussed in Section 5 and we do not want to include it again in the present discussion. The term  $\psi_0 f_1$  describes the transverse excitations driven by the transverse impedance only. This term will be included in the  $\psi_1 f_1$  term if we retain the azimuthal  $m = 0$  longitudinal mode. For this reason, the bunch distribution  $\Psi$  in the combined longitudinal-transverse phase space contains only two terms

$$\Psi(r, \phi; r_\beta, \theta) = \psi_0(r) f_0(r_\beta) + \psi_1(r, \phi) f_1(r_\beta, \theta) e^{-i\Omega s/v} , \quad (6.11)$$

where we have separated out the collective angular frequency from  $\psi_1 f_1$ .

In the circular coordinates, the linearized Vlasov equation becomes

$$\left[ -i\frac{\Omega}{v}f_1\psi_1 + \frac{\omega_s}{v}f_1\frac{\partial\psi_1}{\partial\phi} + \frac{\omega_\beta}{v}\psi_1\frac{\partial f_1}{\partial\theta} \right] e^{-i\Omega s/v} - \psi_0\frac{df_0}{dr_\beta}\sin\theta\frac{c}{E_0\omega_\beta\beta}\langle F_1^\perp(\tau; s) \rangle = 0. \quad (6.12)$$

It is worth pointing out that since the transverse wake force  $\langle F_1^\perp(\tau; s) \rangle$  is a function of the longitudinal coordinate  $\tau$ , it should also contribute to the second equation of Eq. (5.2) although the longitudinal wake force has been neglected here. It is, however, legitimate to drop this contribution if synchro-betatron resonance is avoided and the transverse beam size has not grown too large. See Exercise 6.4.

The next approximation is to consider only the rigid dipole mode in the transverse phase space; i.e., the bunch is displaced by an infinitesimal amount  $D$  from the center of the transverse phase space and executes betatron oscillations by revolving at frequency  $\omega_\beta/(2\pi)$ . Then we must have

$$f_1(r_\beta, \theta) = -Df'_0(r_\beta)e^{i\theta}. \quad (6.13)$$

Equation. (6.12) then becomes

$$\left[ i(\Omega - \omega_\beta)\psi_1 - \omega_s\frac{\partial\psi_1}{\partial\phi} \right] De^{-i\Omega s/v} + \frac{ic^2}{2E_0\omega_\beta}\psi_0\langle F_1^\perp(\tau; s) \rangle = 0, \quad (6.14)$$

where we have dropped the  $e^{-i\theta}$  component of  $\sin\theta$  because that corresponds to rotation in the transverse phase space with frequency  $-\omega_\beta/(2\pi)$  which is very far from  $\omega_\beta/(2\pi)$  provided that the frequency shifts due to the wake force is small.

The transverse wake force on a beam particle in the  $n$ -th bunch at a time advance  $\tau$  is, similar to the longitudinal counterpart in Eq. (5.9),

$$\langle F_{1n}^\perp(\tau; s) \rangle = \frac{e^2D}{C} \sum_{k=-\infty}^{\infty} \sum_{\ell=0}^{M-1} \int_{-\infty}^{\infty} d\tau' \rho_\ell[\tau'; s - kC - (s_\ell - s_n) - v(\tau' - \tau)] W_1[kC + (s_\ell - s_n) + v(\tau' - \tau)]. \quad (6.15)$$

We assume  $M$  identical bunches equally spaced. For the  $\mu$ -th coupled mode, we substitute in the above expression the perturbed density of the  $n$ -th bunch  $\rho_{1n}(\tau)e^{-i\Omega s/v}$  including the phase lead as given by Eq. (5.10). Now the derivation is exactly similar to the longitudinal counter part and we obtain

$$\langle F_{1n\mu}^\perp(\tau; s) \rangle = \frac{ie^2MD\omega_0\beta}{C} e^{-i\Omega s/v} \sum_{q=-\infty}^{\infty} \tilde{\rho}_{1n}(\omega_q) Z_1^\perp(\omega_q) e^{i\omega_q\tau}, \quad (6.16)$$

where  $\omega_q = (qM + \mu)\omega_0 + \omega_\beta + \Omega$ . We next substitute the result into the linearized Vlasov equation and expand  $\psi_1$  into azimuthals according to  $\psi_1(r, \phi) = \sum_m \alpha_m R_m(r) e^{im\phi}$ . We finally obtain Sacherer integral equation for transverse instability

$$(\Omega - \omega_\beta - m\omega_s)\alpha_m R_m(r) = -\frac{i\pi e^2 MNc}{E_0\omega_\beta T_0^2} g_0 \sum_{m'} i^{m-m'} \alpha_{m'} \int r' dr' R_{m'}(r') \sum_q Z_1^\perp(\omega_q) J_{m'}(\omega_q r') J_m(\omega_q r), \quad (6.17)$$

where the unperturbed distribution  $g_0(r)$  defined in Eq. (5.26) has been used instead of  $\psi_0(r)$ . Notice that all transverse distributions are not present in the equation and what we have are longitudinal distributions. This is not unexpected because we have retained only one transverse mode of motion, namely the rigid

dipole mode, in the transverse phase space. Therefore the Sacherer integral equation for transverse instability is almost the same as the one for longitudinal instability. There are only two differences. First, the unperturbed longitudinal distribution  $g_0(r)$  appears in the former but  $r^{-1}dg_0(r)/dr$  appears in the latter. Second, although the  $m=0$  mode does not occur in the longitudinal equation because of violation of energy conservation, however, it is a valid azimuthal mode in the transverse equation because it describes rigid betatron oscillation.

## 6.2 SOLUTION OF SACHERER INTEGRAL EQUATIONS

Consider first the transverse integral equation, where  $W(r) = g_0(r)$  is considered to be a weight function. Find a complete set of orthonormal functions  $g_{mk}(r)$  ( $k = 1, 2, \dots$ ) such that

$$\int W(r)g_{mk}(r)g_{m'k'}(r)rdr = \delta_{kk'} . \quad (6.18)$$

On both sides of the integral equation, do the expansion

$$\alpha_m R_m(r)e^{im\phi} = \sum_k a_{mk} W(r)g_{mk}(r)e^{im\phi} . \quad (6.19)$$

Multiply on both sides by  $W(r)g_{mk}(r)$  and integrate over  $rdr$ . We obtain from Eq. (6.17),

$$(\Omega - \omega_\beta - m\omega_s)a_{mk} = -\frac{i\pi e^2 M N c}{E_0 \omega_\beta T_0^2} \sum_{m'k'} a_{m'k'} \sum_q Z_1^\perp(\omega_q) \tilde{\lambda}_{mk}^*(\omega_q) \tilde{\lambda}_{m'k'}(\omega_q) , \quad (6.20)$$

where we have defined

$$\tilde{\lambda}_{mk}(\omega) = \int i^{-m} W(r) J_m(\omega r) g_{mk}(r) r dr . \quad (6.21)$$

The  $\tilde{\lambda}_{mk}(\omega)$  is the Fourier transform of the eigen-mode  $\lambda_{mk}(\tau)$ , which can be shown to be in fact a linear density. We start with the Fourier transform of the linear density of the  $mk$ -th mode

$$\tilde{\rho}_{(mk)}(\omega) = \frac{1}{2\pi} \int d\tau \rho_{(mk)}(\tau) e^{-i\omega\tau} = \frac{1}{2\pi} \int d\tau d\Delta E \psi_{(mk)}(\tau, \Delta E) e^{-i\omega\tau} . \quad (6.22)$$

Now substitute the  $mk$ -th mode in Eq. (6.19) for  $\psi_{(mk)}$  and obtain

$$\tilde{\rho}_{(mk)}(\omega) = \frac{\omega_s \beta^2 E_0}{2\pi\eta} \int r dr d\phi W(r) g_{mk}(r) e^{im\phi - i\omega\tau} . \quad (6.23)$$

The integration over  $\phi$  can be performed to yield a Bessel function. Finally using the definition of  $\tilde{\lambda}_{mk}(\omega)$  given in Eq. (6.21), we arrive at

$$\tilde{\rho}_{(mk)}(\omega) = \frac{\omega_s \beta^2 E_0}{\eta} \int r dr W(r) g_{mk}(r) i^{-m} J_m(\omega r) = \frac{\omega_s \beta^2 E_0}{\eta} \tilde{\lambda}_{mk}(\omega) . \quad (6.24)$$

Taking the Fourier transform, we therefore obtain

$$\rho_{(mk)}(\tau) = \frac{\omega_s \beta^2 E_0}{\eta} \lambda_{mk}(\tau) . \quad (6.25)$$

Notice that  $\tilde{\lambda}_{mk}(\omega)$  is dimensionless; therefore it must be a function of  $\omega\tau_L$  where  $\tau_L$  is the total bunch length. The sum over the power spectrum should give us

$$\sum_q |\tilde{\lambda}_{mk}(\omega)|^2 \approx \int \frac{d\omega}{M\omega_0} |\tilde{\lambda}_{mk}(\omega)|^2 \sim \frac{1}{M\omega_0\tau_L} . \quad (6.26)$$

For this reason, Eq. (6.20) can roughly be transformed into

$$(\Omega - \omega_\beta - m\omega_s)a_{mk} = -\frac{i}{1+m} \frac{e\beta c^2}{2\omega_\beta E_0} \frac{I_b}{L} \sum_{m'k'} a_{m'k'} \frac{\sum_q Z_1^\perp(\omega_q) \tilde{\lambda}_{mk}^*(\omega_q) \lambda_{m'k'}(\omega_q)}{\sum_q \tilde{\lambda}_{mk}^*(\omega_q) \lambda_{mk}(\omega_q)}, \quad (6.27)$$

which is especially useful if we include only one mode of excitation. For example, the lowest radial mode  $k = 1$  is usually the most prominent one to be excited and the different azimuthal modes do not mix when the perturbation is small.

This expression is very similar to the coasting-beam formula of Eq. (6.2). Besides the averaging over the power spectra, the coasting beam current per unit length  $I_0/C$  is replaced by the average single bunch current  $I_b$  divided by the total bunch length  $L$  in meters. The factor  $(1+m)^{-1}$  in front says that higher-order modes are harder to excite, and is introduced under some assumption of the unperturbed distribution in phase space [15]. It is easy to understand why the power spectrum  $h_{mk}(\omega) = |\tilde{\lambda}_{mk}(\omega)|^2$  enters because  $Z_1^\perp(\omega) \tilde{\lambda}_{mk}(\omega)$  gives the deflecting field, which must be integrated over the bunch spectrum to get the total force. Written in the form of Eq. (6.27), there is no need for  $\tilde{\lambda}_{mk}(\omega)$  or  $\lambda_{mk}(\tau)$  to have any special normalization.

The Sacherer longitudinal integral equation (5.25) can be solved in exactly the same way by identifying the weight function as

$$W(r) = -\frac{1}{r} \frac{dg_0(r)}{dr}, \quad (6.28)$$

where the negative sign is included because  $dg_0(r)/dr < 0$ . The result is

$$(\Omega - m\omega_s)a_{mk} = \frac{i2\pi e^2 MNm\eta}{\beta^2 E_0 T_0^2 \omega_s} \sum_{m'k'} a_{m'k'} \sum_q \frac{Z_0^\parallel(\omega_q)}{\omega_q} \tilde{\lambda}_{mk}^*(\omega_q) \tilde{\lambda}_{m'k'}(\omega_q), \quad (6.29)$$

where  $\tilde{\lambda}_{mk}(\omega_q)$  is again given by Eq. (6.21), but with the weight function replaced by Eq. (6.28). However, these  $\tilde{\lambda}_{mk}(\omega_q)$  have the dimension of of (time) $^{-1}$  because the weight function is different. Dimensional analysis gives

$$\sum_q |\tilde{\lambda}_{mk}(\omega)|^2 \approx \int \frac{d\omega}{M\omega_0} |\tilde{\lambda}_{mk}(\omega)|^2 \sim \frac{1}{M\omega_0 \tau_L^3}. \quad (6.30)$$

Equation (6.29) becomes approximately

$$(\Omega - m\omega_s)a_{mk} = \frac{im}{1+m} \frac{4\pi^2 e I_b \eta}{3\beta^2 E_0 \omega_s \tau_L^3} \sum_{m'k'} a_{m'k'} \frac{\sum_q \frac{Z_0^\parallel(\omega_q)}{\omega_q} \tilde{\lambda}_{m'k'}(\omega_q) \tilde{\lambda}_{mk}^*(\omega_q)}{\sum_q \tilde{\lambda}_{mk}^*(\omega_q) \tilde{\lambda}_{mk}(\omega_q)}, \quad (6.31)$$

where the extra factor in front is a result of the assumption of some particular unperturbed phase-space distribution [15].

Some comments are necessary. From Eq. (6.18), it appears that the orthonormal functions  $g_{mk}(r)$  depends on the weight function  $W(r)$  only and is independent of the azimuthal  $m$ . As a result,  $g_{mk}(r)$  will not be uniquely defined. In fact, this is not true. If we look into either the Sacherer's longitudinal integral equation (5.27) or the transverse integral equation (6.17) for one single azimuthal, it is easy to see that

$$R_m(r) \propto W(r) J_m(\omega_q r). \quad (6.32)$$

Therefore, for small  $r$ , we must have the behavior

$$R_m(r) \sim r^m \lim_{r \rightarrow 0} W(r). \quad (6.33)$$

Taking the parabolic distribution in the longitudinal case as an example,  $\lim_{r \rightarrow 0} W(r)$  is a constant implying that  $R_m(r) \sim r^m$ . From Eq. (6.19), since  $g_{mk}(r)$  is the expansion of  $R_m(r)$ , the small- $r$  behavior of  $g_{mk}(r)$  will be constrained. This makes the set of orthonormal functions  $g_{mk}(r)$  dependent on the azimuthal  $m$  and become, in fact, unique.

### 6.3 SACHERER SINUSOIDAL MODES

Assuming the perturbation is small so that only a single azimuthal mode will contribute, we learn from the Sacherer integral equation (6.17) that the perturbed excitation is

$$R_m(r)e^{im\phi} \propto W(r)J_m(\omega_r r)e^{im\phi} . \quad (6.34)$$

For a bunch of half length  $\hat{\tau} = \frac{1}{2}\tau_L$ ,  $R_m(\hat{\tau}) = 0$ . So it is reasonable to write the  $k$ -th radial mode corresponding to azimuthal  $m$  as

$$R_{mk}(r)e^{im\phi} \propto W(r)J_m\left(x_{mk}\frac{r}{\hat{\tau}}\right)e^{im\phi} , \quad (6.35)$$

where  $x_{mk}$  is the  $k$ -th zero of the Bessel function  $J_m$ . Sacherer [17] discovered that, assuming a uniform or water-bag unperturbed distribution; i.e.,  $W(r)$  is constant for  $r < \hat{\tau}$ , the projection of  $R_{mk}(r)e^{im\phi}$  onto the  $\tau$  axis

$$\rho_{(mk)}(\tau) \propto \int W(r)J_m\left(x_{mk}\frac{r}{\hat{\tau}}\right)e^{im\phi}d\Delta E \quad (6.36)$$

is approximately sinusoidal. In fact, head-tail excitations that are sinusoidal-like had been observed in the CERN PS booster. For this reason, instead of solving the integral equation, Sacherer approximated  $\rho_{(mk)}(\tau)$  by a linear combination of sinusoidal functions, and these modes are called sinusoidal modes. He introduced a set of orthonormal functions

$$\lambda_m(\tau) \propto \begin{cases} \cos(m+1)\pi\frac{\tau}{\tau_L} & m = 0, 2, \dots, \\ \sin(m+1)\pi\frac{\tau}{\tau_L} & m = 1, 3, \dots. \end{cases} \quad (6.37)$$

Note that  $\lambda_m(\tau)$  has exactly  $m$  nodes along the bunch not including the two ends. If we restrict ourselves to the most prominent lowest radial mode ( $k = 1$ ), these  $\lambda_m(\tau)$ 's are just the approximates to  $\rho_{(m1)}(\tau)$ . From now on, the radial mode index  $k$  will be dropped.

The power spectrum of the modes in Eq. (6.37) is proportional to

$$h_m(\omega) = \frac{4(m+1)^2}{\pi^2} \frac{1 + (-1)^m \cos \pi y}{[y^2 - (m+1)^2]^2} \quad (6.38)$$

where  $y = \omega\tau_L/\pi$  and  $\tau_L = L/v$  is the total length of the bunch in time. They are plotted in Fig. 12. The normalization of  $h_m(\omega)$  in Eq. (6.38) has been chosen in such a way that, when the smooth approximation is applied to the summation over  $k$ , we have

$$B \sum_{k=-\infty}^{+\infty} h_m(\omega) \approx \frac{B}{M\omega_0} \int_{-\infty}^{+\infty} h_m(\omega)d\omega = 1 . \quad (6.39)$$

Here  $B = M\omega_0\tau_L/(2\pi)$  is the bunching factor for  $M$  identical equally-spaced bunches, or the ratio of full bunch length to bunch separation.

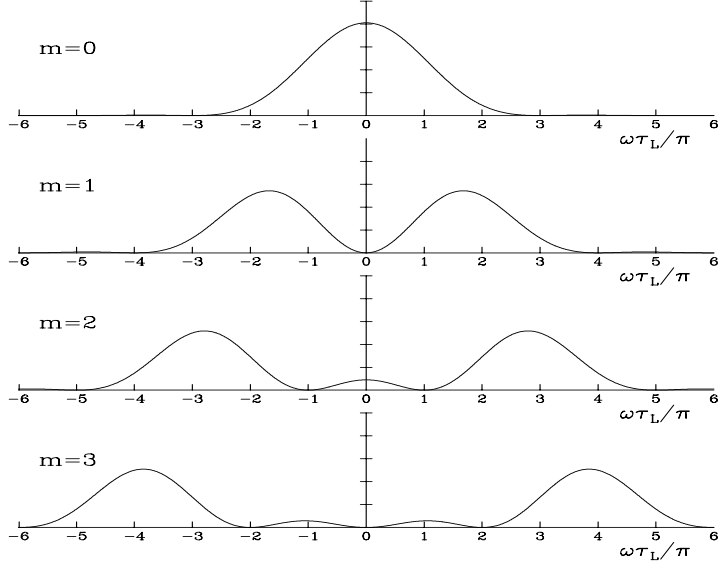


Figure 12: Power spectra  $h_m(\omega)$  for modes  $m = 0$  to 3 with zero chromaticity.

For distribution  $g_0(r) \propto (\hat{\tau}^2 - r^2)^{-1/2}$  in the longitudinal phase space so that the linear density becomes constant, the spectral excitations of the lowest radial mode  $\lambda_m(\tau)$  are the Legendre polynomials, the Fourier transform  $\tilde{\lambda}_m(\omega)$  are the spherical Bessel functions  $j_m$ , and the power spectra  $h_m \propto |j_m|^2$ . We called these the Legendre modes. For a bi-Gaussian distribution in the longitudinal phase space,  $\lambda_m(\tau)$  are the Hermite polynomials and  $\tilde{\lambda}_m(\omega)$  are  $\omega^m$  multiplied by a Gaussian. We call these the Hermite modes.

For the longitudinal integral equation, we have the same modes if we have the same weight function. For the longitudinal case, the weight function is  $W(r) = g'_0(r)/r$  instead. Therefore the sinusoidal modes correspond to  $g_0(r) \propto (\hat{\tau}^2 - r^2)$  or linear density  $\rho(\tau) \propto (\hat{\tau}^2 - \tau^2)^{3/2}$ . The Legendre modes correspond to  $g_0(r) \propto (\hat{\tau}^2 - r^2)^{1/2}$  or parabolic linear density  $\rho(\tau) \propto (\hat{\tau}^2 - \tau^2)$ . The Hermite modes correspond to the same bi-Gaussian distribution as in the transverse situation.

Sometimes the growth rates computed are rather sensitive to the longitudinal bunch distribution assumed. Therefore, results using the sinusoidal modes are estimates only.

## 6.4 CHROMATICITY FREQUENCY SHIFT

The betatron tune  $\nu_\beta$  of a beam particle depends on its momentum offset  $\delta$  through the chromaticity  $\xi$ , which is a property of the lattice of the accelerator and is defined as<sup>†</sup>

$$\Delta\nu_\beta = \xi\delta, \quad (6.40)$$

Because the beam particle makes synchrotron oscillation, the betatron phase is continuously slipping. We would like to compute the phase slip for a particle that has a time advance  $\tau$  relative to the synchronous particle.

<sup>†</sup>Sometimes, especially in Europe, the chromaticity  $\xi$  is also defined by  $\Delta\nu_\beta = \xi\nu_\beta\delta$ .

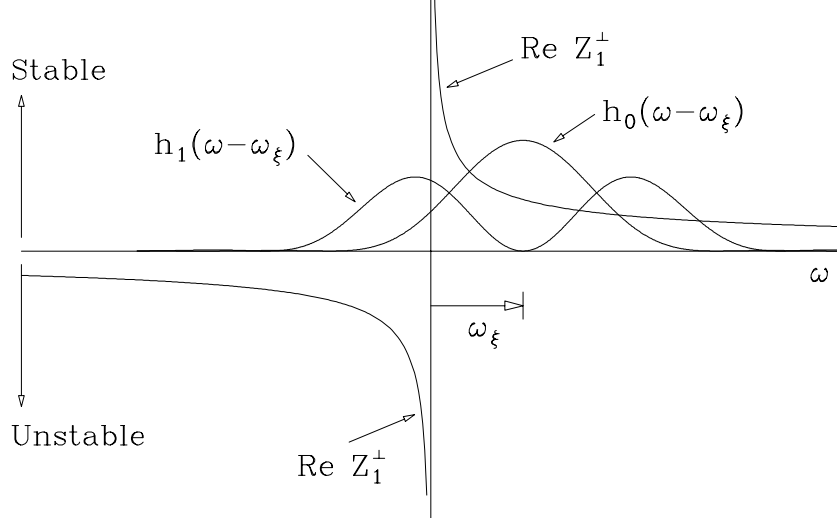


Figure 13: Positive chromaticity above transition shifts the all modes of excitation towards the positive frequency side by  $\omega_\xi$ . Mode  $m = 0$  becomes stable, but mode  $m = 1$  may be unstable because it samples more negative  $\mathcal{R}e Z_1^\perp$  than positive  $\mathcal{R}e Z_1^\perp$ .

The momentum offset in Eq. (6.40) can be eliminated using the equation of motion of the phase

$$\Delta\tau = -\eta T_0 \delta, \quad (6.41)$$

where  $\eta$  is the slip factor and  $\Delta\tau$  is the change in time advance of the particle in a turn. The phase lag in a turn is then

$$\int 2\pi \Delta\nu_\beta = -2\pi \frac{\xi}{\eta} \int \frac{\Delta\tau}{T_0} = -\frac{\xi\omega_0}{\eta} \tau. \quad (6.42)$$

This means that the phase lag increases linearly along the bunch and is independent of the momentum offset. For a bunch of half length  $\hat{\tau}$ , the tail of the bunch,  $\tau = -\hat{\tau}$ , lags the head of the bunch,  $\tau = +\hat{\tau}$ , by the phase  $2\hat{\tau}\omega_\xi$ , where

$$\omega_\xi = \frac{\xi\omega_0}{\eta} \quad (6.43)$$

is called the betatron angular frequency shift due to chromaticity. For this reason,  $\omega_\xi$  should be subtracted from  $\omega_p$  in the argument of the power spectrum in Eqs. (6.20) and (6.27).

For positive chromaticity above transition,  $\omega_\xi > 0$ . The modes of excitation in Fig. 12 are therefore shifted to the right by the angular frequency  $\omega_\xi$ . As shown in Fig. 13, mode  $m = 0$  sees more impedance in positive frequency than negative frequency and is therefore stable. However, it is possible that mode  $m = 1$ , as in Fig. 13, samples more the highly negative  $\mathcal{R}e Z_1^\perp$  at negative frequencies than positive  $\mathcal{R}e Z_1^\perp$  at positive frequencies and becomes unstable.

## EXERCISES

- 6.1. Fill in all the steps in the derivation of Sacherer integral equation for transverse instabilities.
- 6.2. Derive the power spectra of the sinusoidal modes of excitation in Eq. (6.37), and show that they are given by Eq. (6.38) when properly normalized according to Eq. (6.39).

- 6.3. If the transverse impedance is sufficiently smooth, it can be removed from the summation in Eq. (6.27). Show that the growth rate for the  $m = 0$  mode becomes

$$\frac{1}{\tau_0} = -\frac{eI_b c}{2\omega_\beta E_0 \tau_L} \operatorname{Re} Z_1^\perp(\omega_\xi) . \quad (6.44)$$

The transverse impedance of the CERN PS had been measured in this way by recording the growth rates of a bunch at different chromaticities. The CERN PS had a mean radius of 100 m and could store proton bunches from 1 to 26 GeV with a transition gamma of  $\gamma_t = 6$ . The bunch had a spectral spread of  $\sim \pm 100$  MHz, implying that the each measurement of the impedance was averaged over an interval of  $\sim 200$  MHz. If the impedance had to be measured up to  $\sim 2$  GHz and the sextupoles in the PS could attain chromaticities in the range of  $\pm 10$ , at what proton energy should this experiment be carried out?

- 6.4. Redefine the longitudinal coordinates in Eq. (5.1) by  $X = xv$  and  $P_x = p_x v$  so that  $X$  carries the dimension of length.

(a) Show that, for the equations of motion (5.2) in the longitudinal phase space and (6.4) in the transverse phase space, the Hamiltonian is

$$H = -\frac{\omega_s}{2v}(X^2 + P_x^2) - \frac{\omega_\beta}{2v}(y^2 + p_y^2) + \frac{v\eta}{E_0\omega_s\beta^2} \int_0^X dX' \langle F_0^\parallel(X'/v; s) \rangle + \frac{cy}{E_0\omega_\beta\beta^2} \langle F_1^\perp(X/v; s) \rangle . \quad (6.45)$$

(b) Show that the second equation of motion in Eq. (5.2) needs to be modified to

$$\frac{dp_x}{ds} = \frac{\omega_s}{v}x - \frac{\eta}{E_0\omega_s\beta^2} \langle F_0^\parallel(x; s) \rangle - \frac{y}{E_0\omega_\beta\beta^3 v} \frac{\partial}{\partial x} \langle F_1^\perp(x; s) \rangle , \quad (6.46)$$

where the last term is the synchro-betatron coupling term which we dropped in our discussion.

## 7 TRANSVERSE COUPLED-BUNCH INSTABILITIES

### 7.1 RESISTIVE WALL

If there are  $M$  identical equally spaced bunches in the ring, there are  $\mu = 0, \dots, M-1$  transverse coupled modes when the centers-of-mass of one bunch leads its predecessor by the betatron phase of  $2\pi\mu/M$ . The betatron tune shift for the  $\mu$ -th coupled-bunch mode is exactly the same as the formula in Eq. (6.27) except for the replacement of  $\omega_p$  by  $\omega_q = (qM + \mu)\omega_0 + \omega_\beta + m\omega_s$ ; i.e.,

$$\Delta\omega_{m\mu} = -\frac{i}{1+m} \frac{eMI_b c}{4\pi\nu_\beta E_0} \frac{\sum_q Z_1^\perp(\omega_q) h_m(\omega_q - \chi/\tau_L)}{B \sum_q h_m(\omega_q - \chi/\tau_L)} , \quad (7.1)$$

where the bunching factor  $B = ML/C$  has been used and  $\chi = \omega_\xi \tau_L$  is the chromaticity phase shift across the bunch.

A most serious transverse coupled-bunch instability that occurs in nearly all storage rings is the one driven by the resistive wall. Since  $\operatorname{Re} Z_1^\perp \propto \omega^{-1/2}$  and is positive (negative) when  $\omega$  is positive (negative), a small negative frequency betatron line, which acts like a narrow resonance, can cause coupled-bunch instability. Take, for example, the Tevatron in the fixed target mode, where there are  $M = 1113$  equally spaced bunches. The betatron tune is  $\nu_\beta = 19.6$ . The lowest negative betatron frequency line is at

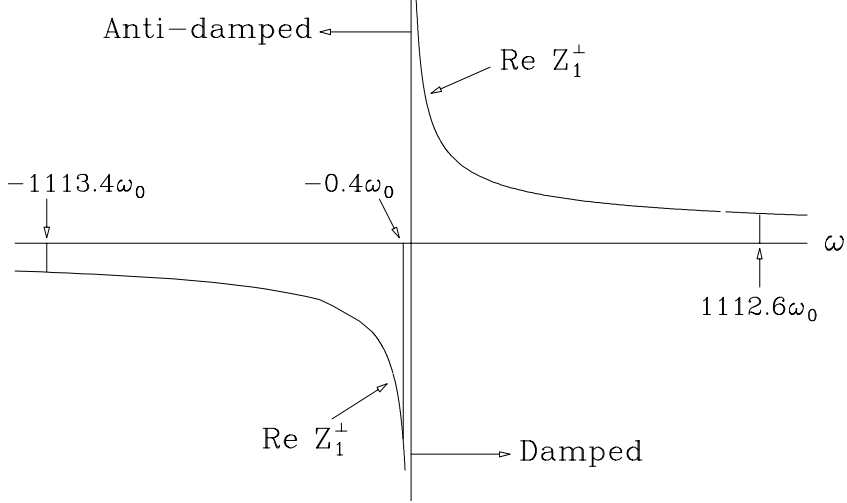


Figure 14: The  $-0.4\omega_0$  betatron line in the Tevatron dominates over all other betatron lines for  $\mu = 1093$  mode coupled-bunch instability driven by the resistive wall impedance.

$(qM + \mu)\omega_0 + \omega_\beta = -0.4\omega_0$ , for mode  $\mu = 1093$  and  $q = -1$ . The closet damped betatron line ( $q = 0$ ) is at  $(1113 - 0.4)\omega_0$ , but  $\text{Re } Z_1^\perp$  is only  $-\sqrt{0.4/1112.6}$  the value at  $-0.4\omega_0$ . The next anti-damped betatron line ( $q = -2$ ) is at  $-1113.4\omega_0$ , with  $\text{Re } Z_1^\perp$  equal to  $\sqrt{0.4/1113.4}$  the value at  $-0.4\omega_0$ . This is illustrated in Fig. 14. Thus it is only the  $-0.4\omega_0$  betatron line that dominates. From Eq. (7.1), the growth rate for this mode can therefore be simplified to

$$\frac{1}{\tau_{m\mu}} \approx -\frac{1}{1+m} \frac{eMI_b c}{4\pi\nu_\beta E_0} \text{Re } Z_1^\perp(\omega_q) F'_m(\omega_q \tau_L - \chi), \quad (7.2)$$

where  $\chi = \omega_\xi \tau_L$  and the form factor is

$$F'_m(\omega \tau_L) = \frac{2\pi h_m(\omega)}{\tau_L \int_{-\infty}^{\infty} h_m(\omega) d\omega}, \quad (7.3)$$

and is plotted in Fig. 15. For zero chromaticity, only the  $m = 0$  mode can be unstable because the power spectra for all the  $m \neq 0$  modes are nearly zero near zero frequency. Since the perturbing betatron line is at extremely low frequency, we can evaluate the form factor at zero frequency. For the sinusoidal modes, we get  $F'(0) = 8/\pi^2 = 0.811$ . One method to make this mode less unstable or even stable is by introducing positive chromaticity when the machine is above transition. For the Tevatron,  $\eta = 0.0028$ , total bunch length  $\tau_L = 5$  ns, revolution frequency  $f_0 = 47.7$  kHz, a chromaticity of  $\xi = +10$  will shift the spectra by the amount  $\omega_\xi \tau_L = 2\pi f_0 \xi \tau_L / \eta = 5.4$ . The form factor and thus the growth rate is reduced by more than 4 times. However, from Figs. 12 and 13, we see that the spectra are shifted by  $\omega_\xi \tau_L / \pi = 1.7$  and the  $m = 1$  mode becomes unstable. Another method for damping is to introduce a betatron angular frequency spread using octapoles, with the spread larger than the growth rate. A third method is to employ a damper. Since this growth is at a very low frequency, we only need a damper with a very narrow bandwidth. Usually the adjacent modes  $\mu = 1092, 1091, \dots$  will also be unstable at the  $-1.4\omega_0, -2.4\omega_0, \dots$  betatron line; but the growth rates will be smaller.

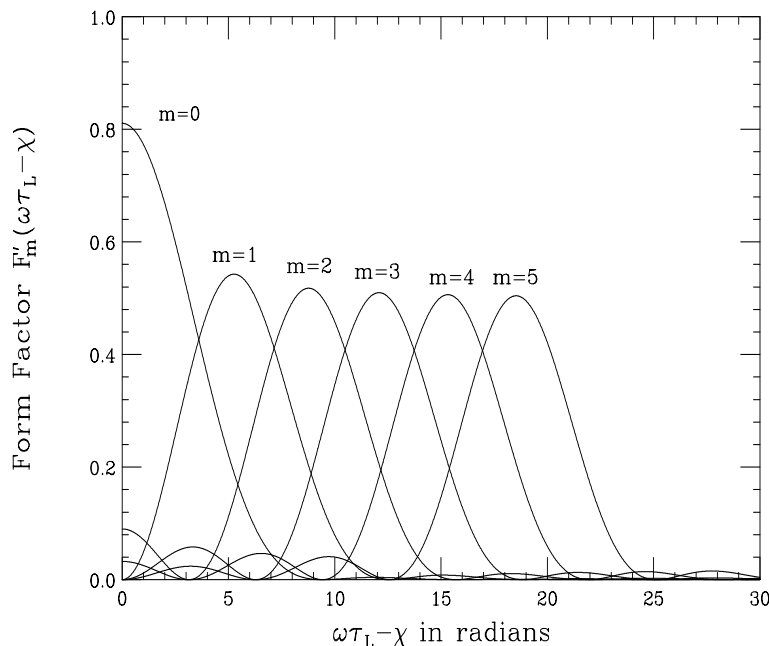


Figure 15: Plot of form factor  $F'_m(\omega\tau_L - \chi)$  for modes  $m = 0$  to 5. With the normalization in Eq. (6.39), these are exactly the power spectra  $h_m$ .

## 7.2 NARROW RESONANCES

The narrow higher-order transverse resonant modes of the rf cavities will also drive transverse coupled-bunch instabilities. The growths rate are described by the general growth formula of Eq. (7.1). When the resonance is narrow enough, only the betatron line closest to the resonant frequency  $-\omega_r/(2\pi)$  contributes in the summation. The growth rate is therefore given by Eq. (7.2). Similar to the situation of longitudinal coupled-bunch instabilities, mode  $\mu = 0$  and mode  $\mu = M/2$  if  $M$  is even receive contributions from both the positive-frequency side and negative-frequency side. In the language of only positive frequencies, there are the upper and lower betatron side-bands flanking each revolution harmonic line. The lower side-band originates from negative frequency and is therefore anti-damped. For these two modes, both the upper and lower side-bands correspond to the same coupled-bunch mode. If the resonant frequency of the resonance leans more towards the lower side band, there will be a growth. If the resonant frequency leans more towards the upper side band, there will be damping. This is the Robinson's stability analog in the transverse phase plane. There is one important difference between transverse coupled-bunch instabilities driven by the resistive-wall impedance and by the higher-order resonant modes. The former is at very low frequency and therefore the form factor  $F_1$  is close to 1 when the chromaticity is zero. The latter, however, is at the high frequency of the resonances. The form factor usually assumes a much smaller value and we sometimes refer this to “damping” from the spread of the bunch.

## EXERCISES

- 7.1. For the example of resistive-wall driven coupled-bunch instability of the Tevatron at the fixed target mode, try to sum up the contribution for all frequencies for the  $\mu = 1093$  mode and compare the result of taking only the lowest frequency line.

- 7.2. For the same example in Exercise 7.1, compare the growth rates of mode  $\mu = 1092, 1091, \dots$ , with mode 1093. How many modes do we need to include so that the growth rate drops to below 1/4 of that of mode 1093?
- 7.3. For a narrow resonance that has a total width larger than  $2[\nu_\beta]\omega_0$  where  $[\nu_\beta]$  is the residual betatron tune and the bunch power spectrum is much wider than the revolution frequency, show that the growth rate is given by

$$\frac{1}{\tau_{m\mu}} \approx \frac{eMI_b c}{4\pi\nu_\beta E_0} \frac{h_m(\omega_r - \chi/\tau_L)}{B \sum_{q'} h_m(\omega_{q'} - \chi/\tau_L)} \times \\ \times \{ \text{Re} Z_1^\perp[(q_1 M - \mu - \nu_\beta)\omega_0 - m\omega_s] - \text{Re} Z_1^\perp[(q_2 M + \mu + \nu_\beta)\omega_0 + m\omega_s] \}, \quad (7.4)$$

where  $q_1$  and  $q_2$  are some positive integer so that

$$(q_1 M - \mu - \nu_\beta)\omega_0 \approx \omega_r, \\ (q_2 M + \mu + \nu_\beta)\omega_0 \approx \omega_r. \quad (7.5)$$

Such  $q_1$  and  $q_2$  are possible only when  $\mu = 0$  or  $\mu = M/2$  if  $M$  is even. Therefore whether the coupled-bunch mode is stable or unstable depends on whether the resonance is leaning more towards the upper betatron side-band or the lower betatron side-band.

## 8 HEAD-TAIL INSTABILITIES

Let us now consider the short-range field of the transverse impedance; i.e.,  $Z_1^\perp(\omega)$  when  $\omega$  is large. This is equivalent to replacing the discrete line spectrum by a continuous spectrum. Since  $\text{Re} Z_\perp(\omega)$  is antisymmetric, the summation in Eq. (6.27) or Eq. (7.1) when transformed into an integration will vanish identically at zero chromaticity. There can only be instability when the chromaticity is nonzero. The growth rate for the  $m$ -th azimuthal mode is therefore

$$\frac{1}{\tau_m} = -\frac{1}{1+m} \frac{\pi e c I_b}{E_0 \omega_\beta \omega_0^2 \tau_L^2} \int_{-\infty}^{\infty} d\omega \text{Re} Z_1^\perp(\omega) h_m(\omega - \omega_\xi). \quad (8.1)$$

Note that the factor of  $M$ , the number of bunches, in the numerator and denominator cancel. This is to be expected because the growth mechanism is driven by the short-range wake field and the instability is therefore a single-bunch effect. This explains why the growth rate  $\tau_m^{-1}$  does not contain the the subscript  $m$  describing phase relationship of consecutive bunches.

Let us demonstrate this by using only the resistive wall impedance. We substitute the expression of the resistive wall impedance of Eq. (1.20) into Eq. (8.1). The result of the integration over  $\omega$  is [16]

$$\frac{1}{\tau_m} = -\frac{1}{1+m} \frac{e I_b c}{4\nu_\beta E} \left( \frac{2}{\omega_0 \tau_L} \right)^{1/2} |Z_1^\perp(\omega_0)| F_m(\chi), \quad (8.2)$$

where  $|Z_1^\perp(\omega_0)|$  is the magnitude of the resistive wall impedance at the revolution frequency. The form factor is given by

$$F_m(\chi) = \sqrt{\frac{2}{\pi}} \int_0^\infty \frac{dy}{\sqrt{y}} [h_m(y - y_\xi) - h_m(y + y_\xi)], \quad (8.3)$$

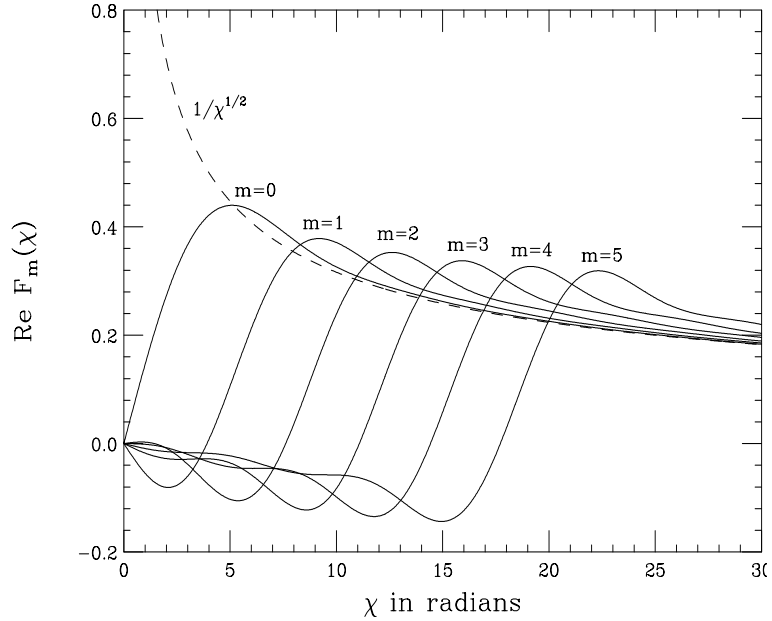


Figure 16: Form factor  $F_m(\chi)$  for head-tail instability for modes  $m = 0$  to 5.

where  $h_m$  are power spectra of the  $m$ -th excitation mode in Eq. (6.37) written as functions of  $y = \omega\tau_L/\pi$  and  $y_\xi = \chi/\pi = \xi\omega_0\tau_L/(\pi\eta)$ . The first term in the integrand comes from contributions by positive frequencies while the second term by negative frequencies. The form factors for  $m = 0$  to 5 are plotted in Fig. 16.

This single-bunch instability will occur in nearly all machines. The  $m = 0$  mode is the rigid-bunch mode when the whole bunch oscillates transversely as a rigid unit. For the  $m = 1$  mode, the head of the bunch moves transversely in one direction while the tail moves transversely in the opposite direction with the center-of-mass stationary, and is called the dipole head-tail mode. This is the head-tail instability first analyzed by Pellegrini and Sands [18, 19].

For small chromaticity  $\xi \lesssim 4$ ,  $\chi \lesssim 2.3$  the integrand in Eq. (8.3) can be expanded and the growth rate becomes proportional to chromaticity. The form factor has been computed listed in Table II, where negative sign implies damping. We see from Table II that mode  $m = 0$  is stable for positive chromaticity. This is expected because the excitation spectrum for this mode has been pushed towards the positive-frequency side. All other modes ( $m > 0$ ) should be unstable because their spectra see relatively more negative  $\text{Re } Z_1^\perp$ . Looking into the form factors in Fig. 16, however, the growth rate for  $m=4$  is tiny and mode  $m=2$  is even stable. This can be clarified by looking closely into the excitation spectra in Fig. 12. We find that while mode  $m = 0$  has a large maximum at zero frequency, all the other higher even  $m$  modes also have small maxima at zero frequency. As these even  $m$  spectra are pushed to the right, these small central maxima see more impedance from positive frequency than negative frequency. Since these small central maxima are near zero frequency where  $|\text{Re } Z_1^\perp|$  is large, their effect may cancel out the opposite effect from the larger maxima which interact with the impedance at much higher frequency where  $|\text{Re } Z_1^\perp|$  is smaller. This anomalous effect does not exist in the Legendre modes or the Hermite modes, because the corresponding power spectra

Table II: Linearized form factor of transverse head-tail modes driven by the resistive wall impedance when  $\chi \lesssim 2.3$ .

Mode	Form Factor
$m$	$F_m$
0	$-0.1495 \chi$
1	$+0.0600 \chi$
2	$-0.0053 \chi$
3	$+0.0191 \chi$
4	$+0.0003 \chi$
5	$+0.0098 \chi$

vanish at zero frequency when  $m > 0$ .

Although the head-tail instabilities can be damped by the incoherent spread in betatron frequency, it is advisable to run the machine at a negative chromaticity above transition. In this case, all the higher modes with  $m \neq 0$  will be stable, and the unstable  $m = 0$  mode can be damped with a damper.

The head-tail instability comes about because of nonzero chromaticity or the betatron tune is a function of energy spread. There is also such an analog in the longitudinal phase space, where the slip factor  $\eta$  is energy-spread dependent. The longitudinal beam distribution then picks up a head-tail phase and instability may arise [21]. In fact, longitudinal head-tail instability had been observed at the CERN SPS [20] and it was also seen at the Fermilab Tevatron.

## EXERCISES

- 8.1. The degrees of freedom of a system are coupled internally. Some degrees of freedom continue to gain energy and grow while some lose energy and are damped. When the system is not getting energy from outside, the sum of the damping or antidamping rates of all degrees of freedom must add up to zero. If the head-tail stability or instability for all azimuthal modes do not draw energy from outside, energy must be conserved, or

$$\sum_{m=0}^{\infty} \frac{1}{\tau_m} = 0, \quad (8.4)$$

where  $\tau_m^{-1}$  is given by Eq. (8.1), independent of chromaticity and the detail of the transverse impedance. Show that Eq. (8.4) is only satisfied if the factor  $(1+m)^{-1}$  in Eq. (8.1) is removed. We may conclude that either the factor  $(1+m)^{-1}$  should not be present in Sacherer formula or this is not an internal system.

Hint: Show that  $\sum_m |h_m(\omega)|^2$  is a constant independent of  $\omega$  by performing the summation numerically. This follows from the fact that the modes of excitation  $\lambda_m(\tau)$  form a complete set. Then the integration over  $\mathcal{Re} Z_1^\perp(\omega_0)$  gives zero.

- 8.2. In an isochronous ring or a linac, the particle at the head of the bunch will not exchange position with the particle at the tail. Thus the particle at the tail suffers from the wake of the head all the time. We can consider a macroparticle model with only two macroparticles each carries charge  $eN/2$  and separated by a distance  $\hat{z}$  longitudinally. The head particle executes a free betatron oscillation

$$y_1(s) = \hat{y} \cos k_\beta s, \quad (8.5)$$

while the tail sees a deflecting wake force  $\langle F_1^\perp \rangle = e^2 N W_1(\hat{z}) y_1(s)/(2\ell)$  and its transverse motion is determined by

$$y_2'' + k_\beta^2 y_2 = -\frac{e^2 N W_1(\hat{z})}{2E_0 \ell}, \quad (8.6)$$

where  $k_\beta = \omega_\beta/v$  is the betatron wave number,  $\ell$  is the length of the vacuum chamber that supplies the wake. If one prefers, one can define  $W_1$  as the wake force integrated over one rf-cavity period; then  $\ell$  will be the length of the cavity period. Show that the solution of Eq. (8.6) is

$$y_2(s) = \hat{y} \left[ \cos k_\beta s - \frac{e^2 N W_1(\hat{z})}{4k_\beta E_0 \ell} s \sin k_\beta s \right]. \quad (8.7)$$

The second term is the resonant response to the wake force and grows linearly. Show that the total growth in transverse amplitude along a length  $\ell_0$  of the linac relative to the head particle is

$$\Upsilon = -\frac{e^2 N W_1(\hat{z}) \ell_0}{4k_\beta E_0 \ell}. \quad (8.8)$$

The above mechanism is called beam breakup.

## 9 MODE-COUPLING

As the beam intensity increases, the shift of each azimuthal mode becomes so big that two adjacent modes overlap each other. The azimuthal mode number is no longer a good eigen-number, and we can no longer represent the perturbation distribution  $\psi_1$  as a single azimuthal mode; instead it should be a linear combination of all azimuthal modes. This phenomenon has been referred to as “mode-coupling,” “strong head-tail,” and “transverse or longitudinal turbulence.”

### 9.1 TRANSVERSE

Let us first consider transverse instability driven by a broad-band impedance. This implies a single bunch mechanism. Also we set the chromaticity to zero. For the  $m$ -th azimuthal mode and  $k$ -th radial mode, Eq. (6.27) or (7.1) becomes

$$(\Omega - m\omega_s)\delta_{mm'}\delta_{kk'} = M_{mm'kk'} \quad (9.1)$$

where, with the aid of Eq. (6.27), the matrix  $M$  is defined as

$$M_{mm'kk'} = -\frac{ieI_b c}{2\omega_\beta E_0 \tau_L} \frac{\int d\omega Z_1^\perp(\omega) \tilde{\lambda}_{m'k'}(\omega) \tilde{\lambda}_{mk}^*(\omega)}{\int d\omega \tilde{\lambda}_{mk}(\omega) \tilde{\lambda}_{mk}^*(\omega)}. \quad (9.2)$$

The summations have been converted to integrations because the impedance is so broad-band that there is no need to distinguish the individual betatron lines. A further simplification is to keep only the first most easily excited radial modes. Then, the problem becomes coupling in the azimuthal modes.

Since  $\Re Z_1^\perp(\omega)$  is odd in  $\omega$  and  $\Im Z_1^\perp(\omega)$  is even in  $\omega$ , only  $\Im Z_1^\perp(\omega)$  will contribute to the diagonal terms of the matrix  $M$  giving only real frequency shifts which will not lead to instability. As the beam current becomes larger, two modes will collide and merge together, resulting in two complex eigen-frequencies, one is

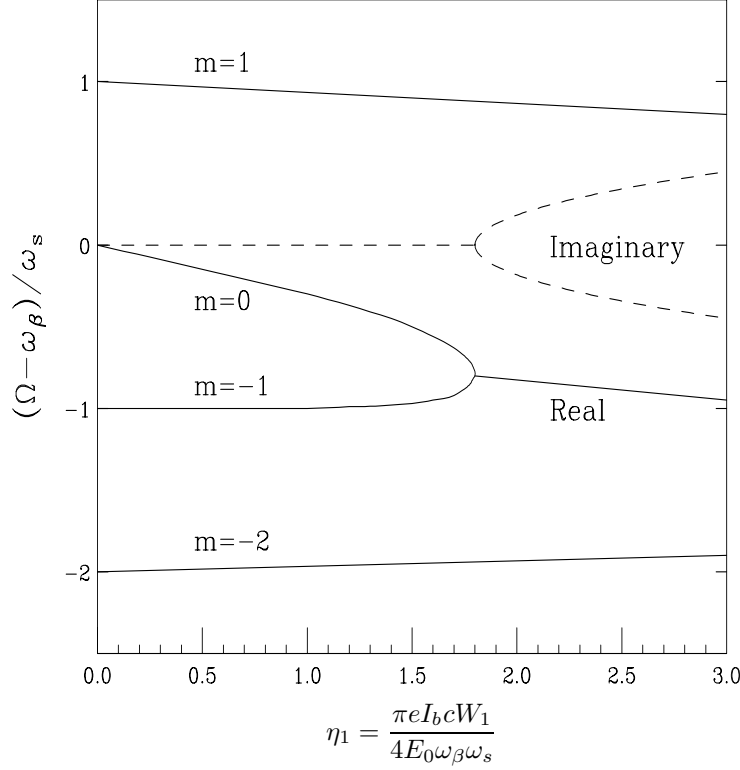


Figure 17: Transverse mode frequencies  $(\Omega - \omega_\beta) / \omega_s$  versus the current intensity parameter  $\eta_1$  for an air-bag bunch distribution perturbed by a constant wake potential  $W_1$ . The instability occurs at  $\eta_1 \approx 1.8$ , when the  $m = 0$  and  $m = 1$  modes collide. The dashed curves are the imaginary part of the mode frequencies or growth/damping rate for the two colliding modes.

the complex conjugate of the other, thus introducing instability. Therefore, coupling should originate from the off-diagonal elements closest to the diagonal. We learn from Eq. (6.37) that the  $m$ -th mode of excitation  $\tilde{\lambda}_m(\omega)$  is even in  $\omega$  when  $m$  is even, and odd in  $\omega$  when  $m$  is odd. Thus, it is  $\Re Z_1^\perp(\omega)$  that gives the coupling.

The eigen-angular-frequencies are solved by

$$\det[(\Omega - \omega_\beta - m\omega_s)I - M] = 0 . \quad (9.3)$$

As an example, an airbag model is perturbed by the impedance

$$Z_1^\perp(\omega) = \frac{W_1}{\omega + i\epsilon} , \quad (9.4)$$

which corresponds to a constant wake function  $W_1$ . The infinite matrix is truncated and the eigenvalues solved numerically. The solution is shown in Fig. 17 [6]. This impedance corresponds to a real part that falls off as frequency increases. The imaginary part is a  $\delta$ -function at zero frequency, and therefore interacts with the  $m = 0$  mode only. This explains why all other modes remain almost unshifted with the exception of  $m = 0$ . The downward frequency shift of the  $m = 0$  mode as the beam intensity increases from zero

is a general behavior for short bunches. The transverse wake force produced by an off-axis beam has the polarity that deflects the beam further away from the pipe axis. This force acts as a defocusing force for the rigid beam mode, and therefore the frequency shifts downward. Such a down shift of the betatron frequency is routinely observed in electron accelerators and serves as an important tool of probing the impedance. Eventually the  $m = 0$  shifts downwards and meets with the  $m = -1$  mode, thus exciting an instability. The threshold is at

$$\eta_1 = \frac{\pi e I_b c W_1}{4 E_0 \omega_\beta \omega_s} \approx 1.8, \quad (9.5)$$

and is bunch-length independent. We can also obtain an approximate threshold from Eqs. (9.1) and (9.2) by equating the frequency shift to  $\omega_s$ , and get

$$\frac{e I_b c Z_1^\perp|_{\text{eff}}}{2 E_0 \omega_\beta \omega_s \tau_L} \approx 1, \quad (9.6)$$

where

$$Z_1^\perp|_{\text{eff}} = \frac{\int d\omega Z_1^\perp(\omega) h_m(\omega)}{\int d\omega h_m(\omega)} \quad (9.7)$$

is called the effective transverse impedance for mode  $m$ . Comparing Eqs. (9.5) and (9.6), we find the two thresholds are almost the same except for the bunch-length dependency, which we think should be understood as follows. Since the imaginary part of the impedance in Eq. (9.4) is a  $\delta$ -function at zero frequency which interacts only with the  $m = 0$  mode. As the bunch length becomes shorter, the spectrum spreads out wider, so that the spectrum at zero frequency becomes smaller. In fact, from Eqs. (6.38) and (6.39), it is clear that  $Z_1^\perp|_{\text{eff}} \propto \tau_L$ , thus explaining why  $\eta_1$  in Eq. (9.5) is bunch-length independent.

Now consider the situation when the impedance is a broad-band resonance. For a very short bunch, the  $m = 0$  mode extends to very high frequencies and will cover part of the high-frequency capacitive part of the resonance. Thus the effective impedance  $Z_1^\perp|_{\text{eff}}$  can become small due to the cancellation of the inductive and capacitive parts. At the same time, the peak of  $\text{Re} Z_1^\perp$  is far from the peak of the  $m = 1$  mode, thus making the coupling between the  $m = 0$  and  $m = 1$  mode very weak. Since the frequency shift is small and the coupling is weak, it will take a much higher beam current for the  $m = 0$  mode to meet with the  $m = 1$  mode, thus pushing up the threshold current. For a long bunch, the  $m = 0$  mode has a small frequency spread. If it stays inside the inductive region where  $\text{Im} Z_1^\perp$  is almost constant,  $Z_1^\perp|_{\text{eff}}$  will be almost constant and the threshold current increase linearly with the bunch length. When the bunch is very long, the  $m = \pm 1$  and even  $m = \pm 2$  and  $m = \pm 3$  modes may stay inside the constant inductive region of the impedance. This implies that the higher azimuthal modes also interact strongly with the impedance and these mode will have large shifts so that the threshold can become much smaller. Several collisions may occur around a small beam-current interval and the bunch can become very unstable suddenly.

The transverse mode-coupling instability was first observed at PETRA and later also at PEP and LEP. The instability is devastating; as soon as the threshold is reached, the bunch disappears.

## 9.2 LONGITUDINAL

The azimuthal modes are not good description of the collective motion of the bunch when the beam current is high enough. Therefore there is also mode-coupling in the longitudinal motion. Similar to the

transverse coupled problem in Eqs. (9.1) and (9.2), we have here

$$(\Omega - m\omega_s)\delta_{mm'}\delta_{kk'} = M_{mm'kk'} \quad (9.8)$$

where, with the aid of Eq. (9.9), the matrix  $M$  is defined as

$$M_{mm'kk'} = \frac{im}{1+m} \frac{4\pi^2 e I_b \eta}{3\beta^2 E_0 \omega_s^2 \tau_L^3} \frac{\int d\omega \frac{Z_0^{\parallel}(\omega)}{\omega} \tilde{\lambda}_{m'k'}(\omega) \tilde{\lambda}_{mk}^*(\omega)}{\int d\omega \tilde{\lambda}_{mk}(\omega) \tilde{\lambda}_{mk}^*(\omega)}, \quad (9.9)$$

where the unperturbed distribution has been assumed to be parabolic. Again here the impedance is broadband so that the discrete summations over the synchrotron side-bands have been replaced by integrals. We have also thrown away all the higher-order radial modes keeping the most easily excited  $k = 0$ . Exactly the same as in the transverse situation, only  $\mathcal{I}m Z_0^{\parallel}(\omega)/\omega$  contributes to the diagonal elements of the coupling matrix and thus to the real frequency shifts of the modes. The coupling of two modes, mostly adjacent, will give instability, which is determined by  $\mathcal{R}e Z_0^{\parallel}(\omega)/\omega$  in the off-diagonal elements next to the diagonal ones. All the discussions about bunch-length dependency on threshold in the transverse case apply here also.

A rough estimate of the threshold can be obtained from Eq. (9.9) by equating the frequency shift to  $\omega_s$ . The threshold is therefore

$$\eta_2 = \frac{4\pi^2 e I_b \eta}{3\beta^2 E_0 \omega_s^2 \tau_L^3} \left. \frac{Z_0^{\parallel}}{\omega} \right|_{\text{eff}} \approx 1, \quad (9.10)$$

where the effective longitudinal impedance for mode  $m$  is defined as

$$\left. \frac{Z_0^{\parallel}}{\omega} \right|_{\text{eff}} = \frac{\int d\omega \frac{Z_0^{\parallel}(\omega)}{\omega} h_m(\omega)}{\int d\omega h_m(\omega)}, \quad (9.11)$$

For convenience, let us introduce a parameter  $x = \omega\tau_L/\pi$ , so that, with the exception of  $m = 0$  which is not an allowed mode in the longitudinal motion, the  $m$ -th mode of excitation peaks at  $x \approx m + 1$  and has a half width of  $\Delta x \approx 1$ . Now consider the Fermilab Main Ring with a revolution frequency 47.71 kHz and total bunch length  $\tau_L \approx 2$  ns. Assume the impedance to be broad-band centered at  $x_r = 7.5$  or  $f_r \sim 1.88$  GHz and quality factor  $Q = 1$ . Numerical diagonalization of the coupling matrix gives frequency shifts as shown in Fig. 18 [22]. We see the first instability occurs when mode  $m = 6$  couples with mode  $m = 7$ , and in the vicinity of the threshold, there are also couplings between modes  $m = 4$  and 5 and modes  $m = 8$  and 9. This happens because the resonance centered at  $x_r = 7.5$  has a half width  $\Delta x_r = x_r/(2Q) = 3.75$ . Thus the  $\mathcal{R}e Z_0^{\parallel}/\omega$  resonant peak encompasses modes  $m = 4$  to 9, which peak at  $x = 5$  to 10. This is a typical picture of mode-coupling instability for long bunches. From the figure, the first instability occurs at

$$\epsilon = \frac{4\pi^2 e I_b \eta}{3\beta^2 E_0 \omega_s^2 \tau_L^3} \frac{R_s}{\omega_r} \approx 0.93. \quad (9.12)$$

On the other hand, the Keil-Schnell criterion of Eq. (4.20) gives a threshold of

$$\frac{e I_b \eta}{\beta^2 E_0 \omega_s^2 \tau_L^3} \frac{R_s}{\omega_r} = \frac{1}{6\pi} \frac{1}{F}, \quad (9.13)$$

where  $F$  is the form factor. This is equivalent to

$$\epsilon = \frac{2\pi}{9} \frac{1}{F}. \quad (9.14)$$

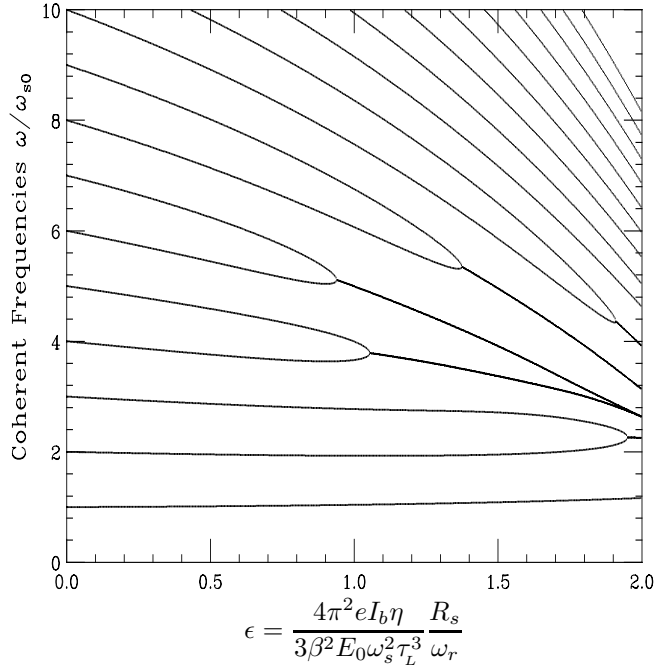


Figure 18: Coupling of modes  $m = 6$  and  $7$  in the presence of a resonance at  $x_r = 7.5$  and  $Q = 1$  above transition.

Thus the mode-coupling threshold is very close to the Keil-Schnell threshold. However, mode-coupling instability is quite different from microwave instability. In the latter, pure reactive impedance can drive an instability; for example, the negative-mass instability just above transition is driven by the space-charge force. It can be demonstrated that pure capacitive impedance will only lead to real frequency shifts of the modes. Although two modes may cross each other, they will not be degenerate to form complex modes. Thus, there is no instability.

When the bunch is short, the modes of excitation spread out to higher frequencies. Therefore when the bunch is short enough, the resonant peak of  $\text{Re} Z_0^{\parallel}/\omega$  resonant peak will encompass only modes  $m = 1$  and  $2$ . Thus, we expect these two modes will collide first to give instability. The  $m = 1$  is the dipole mode and is not shifted at low beam current because the bunch center does not see any reactive impedance. The  $m = 2$  is the quadrupole mode, which is shifted downward above transition. This downshift is a way to measure the reactive impedance of the ring.

When the beam current is above threshold and instability starts, the energy spread increases and so does the bunch length. In an electron ring where there is radiation damping, there is no overshooting and the increase stops when the stability criterion is fulfilled again. The bunch lengthening is therefore determined by the stability criterion. If the bunch samples the impedance at a frequency range where  $Z_0^{\parallel}(\omega) \propto \omega^a$ , the

effective impedance is

$$\left. \frac{Z_0}{\omega} \right|_{\text{eff}} \propto \frac{\int d\omega \omega^{a-1} h_m(\omega)}{\int d\omega h_m(\omega)} \propto \tau_L^{1-a}, \quad (9.15)$$

where use has been made of the fact that the power spectrum  $h_m$  is a function of the dimensionless quantity  $\omega\tau_L$  according to Eq. (6.38) and the result is independent of the functional form of  $h_m$ . From the threshold condition in Eq. (9.10), we have

$$\frac{4\pi^2 e I_b \eta}{3\beta^2 E_0 \omega_s^2 \tau_L^{2+a}} \approx 1. \quad (9.16)$$

Thus the bunch length obeys the scaling criterion of

$$\tau_L \propto \xi^{1/(2+a)}, \quad (9.17)$$

where

$$\xi = \frac{\eta I_b}{\nu_s^2 E_0} \quad (9.18)$$

is the scaling parameter introduced by Chao and Gareyte [12].

Longitudinal mode-coupling is different from transverse mode-coupling. In the latter, the betatron frequency ( $m = 0$ ) is shifted downward to meet with the  $m = -1$  mode. The amount of shift is small, since  $\nu_s/[\nu_\beta] \ll 1$ , where  $[\nu_\beta]$  is the residual betatron tune. Transverse mode-coupling has been measured in many electron rings and the results agree with theory.

In the longitudinal case, the synchrotron quadrupole frequency ( $m = 2$ ) has to be shifted downward to meet with the synchrotron dipole frequency ( $m = 1$ ) and this shift is a 100% of the synchrotron tune. At LEP which is above transition, we expect the synchrotron quadrupole mode to shift downward when the beam current increases from zero. However, it was observed that this mode shifts slightly upward instead. Since the dipole frequency is not shifted, it is hard to visualize how the two modes will be coupled. Some argue that the coupling may not be between two azimuthal modes, but instead between two radial modes that we have discarded in our discussion. But the coupling between two radial modes are generally much weaker. Some say that the actual coupling of the two modes has never been observed experimentally, and the scaling law for bunch lengthening may have been the result of some other theories. Anyway, the theory of longitudinal mode-coupling is far from satisfactory.

## EXERCISES

- 9.1. There is a simple two-particle model to demonstrate transverse mode coupling [6]. Assume the head and tail particles are always separated by  $\hat{z}$  for one half of a synchrotron period  $T_s$  and exchange position for the other half. Similar to Exercise 8.2, we have during  $0 < s/v < T_s/2$ ,

$$\begin{aligned} y_1'' + k_\beta^2 y_1 &= 0, \\ y_2'' + k_\beta^2 y_2 &= -\frac{e^2 N W_1(\hat{z})}{2E_0 C} y_1. \end{aligned} \quad (9.19)$$

(a) Show that the solution is

$$\tilde{y}_1(s) = \tilde{y}_1(0) e^{-ik_\beta s}, \quad (9.20)$$

$$\tilde{y}_2(s) = \tilde{y}_2(0) e^{-ik_\beta s} - i \frac{e^2 N W_1(\hat{z})}{4E_0 C k_\beta} \left[ \frac{\tilde{y}_1^*(0)}{k_\beta} \sin(k_\beta s) + \tilde{y}_1(0) s e^{-ik_\beta s} \right], \quad (9.21)$$

where

$$\tilde{y}_\ell = y_\ell + i \frac{y'_\ell}{k_\beta}, \quad \ell = 1, 2. \quad (9.22)$$

The term with  $\sin(k_\beta s)$  in Eq. (9.21) can be dropped because  $\omega_\beta T_s/2 \ll 1$ . We can therefore write

$$\begin{pmatrix} \tilde{y}_1 \\ \tilde{y}_2 \end{pmatrix}_{s=vT_s/2} = e^{-i\omega_\beta T_s/2} \begin{pmatrix} 1 & 0 \\ i\Upsilon & 1 \end{pmatrix} \begin{pmatrix} \tilde{y}_1 \\ \tilde{y}_2 \end{pmatrix}_{s=0}, \quad (9.23)$$

where

$$\Upsilon = -\frac{\pi e^2 N W_1 v^2}{4 E_0 C \omega_\beta \omega_s}. \quad (9.24)$$

(b) During  $T_s/2 < s/v < T_s$ , show that we have instead

$$\begin{aligned} y_1'' + k_\beta^2 y_1 &= \frac{e^2 N W_1(\hat{z})}{2 E_0 C} y_2, \\ y_2'' + k_\beta^2 y_2 &= 0, \end{aligned} \quad (9.25)$$

so that for one synchrotron period,

$$\begin{pmatrix} \tilde{y}_1 \\ \tilde{y}_2 \end{pmatrix}_{s=vT_s} = e^{-i\omega_\beta T_s} \begin{pmatrix} 1 & i\Upsilon \\ 0 & 1 \end{pmatrix} \begin{pmatrix} 1 & 0 \\ i\Upsilon & 1 \end{pmatrix} \begin{pmatrix} \tilde{y}_1 \\ \tilde{y}_2 \end{pmatrix}_{s=0}. \quad (9.26)$$

(c) Show that the two eigenvalues are

$$\lambda_\pm = e^{\pm i\phi}, \quad \sin \frac{\phi}{2} = \frac{\Upsilon}{2}, \quad (9.27)$$

and stability requires  $\Upsilon \leq 2$ . Compare the result with Eq. (9.5). Note that for a short bunch  $W_1(\hat{z}) < 0$ ; thus  $\Upsilon$  is positive.

9.2. In the two-particle model in Exercise 9.1, if the beam current is slightly above threshold; i.e.,

$$\Upsilon = 2 + \epsilon, \quad (9.28)$$

where  $\epsilon \ll 1$ , compute the complex phase  $\phi$  of the eigenvalues  $\lambda_\pm$ . The growth rate is then

$$\frac{1}{\tau} = \frac{\text{Im} \phi}{T_s} = \frac{2\sqrt{\epsilon}}{T_s}. \quad (9.29)$$

Show that for an intensity 10% above threshold, the growth time is of the order of the synchrotron period.

9.3. For longitudinal mode-coupling, the coupling matrix of Eq. (9.9) can be written as, after keeping only the lowest radial modes,

$$M_{mm'} = \epsilon \omega_s A_{mm'} \quad (9.30)$$

where  $\epsilon$  is given by Eq. (9.12),

$$A_{mm'} = \frac{im}{1+m} \frac{\int d\omega \frac{\omega_r \hat{Z}_0^{\parallel}(\omega)}{\omega} \tilde{\lambda}_{m'}(\omega) \tilde{\lambda}_m^*(\omega)}{\int d\omega \tilde{\lambda}_m(\omega) \tilde{\lambda}_m^*(\omega)}, \quad (9.31)$$

and  $\hat{Z}_0^{\parallel}(\omega)$  has been normalized to the shut impedance  $R_s$ .

If the coupling is not too strong, we can truncate the matrix to  $2 \times 2$  for the coupling between two modes:

$$\begin{vmatrix} \frac{\Omega}{\omega_{s0}} - m - \epsilon A_{mm} & \epsilon A_{mm'} \\ \epsilon A_{m'm} & \frac{\Omega}{\omega_s} - m' - \epsilon A_{m'm'} \end{vmatrix} = 0. \quad (9.32)$$

(a) Show that the collective frequency is given by

$$\Omega = \frac{1}{2}\omega_s \left[ (\nu_m + \nu_{m'}) \pm \sqrt{(\nu_{m'} - \nu_m)^2 + 4\epsilon^2 A_{mm'} A_{m'm}} \right], \quad (9.33)$$

where  $\nu_k = k + \epsilon A_{kk}$ ,  $k = m$  or  $m'$ .

(b) For two adjacent modes ( $m' = m + 1$ ) that are coupled by a resonant peak, the higher-frequency mode samples mostly the capacitive part of the resonance while the lower-frequency mode samples the inductive part. Therefore  $A_{mm} - A_{m'm'} > 0$ . Show that  $A_{mm'} A_{m'm} = -|A_{mm'}|^2$  and the threshold of instability  $\epsilon_{\text{th}}$  is given by

$$|\epsilon_{\text{th}} A_{mm'}| = \frac{1}{2} |\epsilon_{\text{th}} (A_{m'm'} - A_{mm}) - 1|. \quad (9.34)$$

The solution is different depending on whether the bunch energy is above or below transition:

$$\begin{aligned} \epsilon_{\text{th}} &= \frac{1}{2|A_{mm'}| + |A_{m'm'} - A_{mm}|} && \text{above transition,} \\ |\epsilon_{\text{th}}| &= \left| \frac{1}{2|A_{mm'}| - |A_{m'm'} - A_{mm}|} \right| && \text{below transition.} \end{aligned} \quad (9.35)$$

The above shows that the threshold will be higher when the ring is below transition. For this reason, it is advantageous for the ring to be of imaginary  $\gamma_t$  [23].

(c) When the impedance is purely reactive, the next-to-diagonal off-diagonal elements are zero. So we talk about coupling of two modes  $m$  and  $m' = m + 2$  instead. Show that  $A_{mm'} A_{m'm} = |A_{mm'}|^2$  and instability cannot occur.

## References

- [1] W.K.H. Panofsky and W.A. Wenzel, Rev. Sci. Instr. **27**, 967 (1956).
- [2] A.A. Vlasov, J. Phys. USSR **9**, 25 (1945).
- [3] J. Haissinski, Nuovo Cimento **18B**, 72 (1973).
- [4] A.G. Ruggiero, IEEE Trans. Nucl. Sci. **NS-24**, 1205 (1977).
- [5] L.D. Landau, J. Phys. USSR **10**, 25 (1946);
- [6] A.W. Chao, *Physics of Collective Beam Instabilities in High Energy Accelerators*, John Wiley & Sons, 1993, p. 251.
- [7] E. Keil and W. Schnell, CERN Report TH-RF/69-48 (1969); V.K. Neil and A.M. Sessler, Rev. Sci. Instr. **36**, 429 (1965); D. Boussard, CERN Report Lab II/Rf/Int./75-2 (1975).

- [8] S. Krinsky and J.M. Wang, *Particle Accelerators* **17**, 109 (1985).
- [9] J.D. Jackson, *Plasma Phys.* **C1**, 171 (1960).
- [10] R.A. Dory, Thesis, MURA Report 654, 1962.
- [11] Y. Chin and K. Yokoya, *Phys. Rev.* **D28**, 2141 (1983).
- [12] A.W. Chao and J. Gareyte, *Part. Accel.* **25**, 229 (1990).
- [13] P.B. Robinson, *Stability of Beam in Radiofrequency System*, Cambridge Electron Accel. Report CEAL-1010, 1964.
- [14] F.J. Sacherer, *A Longitudinal Stability Criterion for Bunched Beams*, CERN report CERN/MPS/BR 73-1, 1973; *IEEE Trans. Nuclear Sci.* **NS 20**, 3, 825 (1973).
- [15] See for example, J.L. Laclare, *Bunch-Beam Instabilities, —Memorial Talk for F.J. Sacherer*, Proc. 11th Int. Conf. High-Energy Accelerators, Geneva, July 7-11, 1980, p. 526.
- [16] F.J. Sacherer, *Theoretical Aspects of the Behaviour of Beams in Accelerators and Storage Rings*, Proc. First Course of Int. School of Part. Accel., Erice, Nov. 10-22, 1976, p.198.
- [17] F.J. Sacherer, *Methods for Computing Bunched-Beam Instabilities*, CERN Report CERN/SI-BR/72-5, 1972.
- [18] C. Pellegrini, *Nuovo Cimento* **64**, 447 (1969).
- [19] M. Sands, SLAC-TM-69-8 (1969).
- [20] D. Boussard and T. Linnekar, Proc. 2nd EPAC, Nice, 1990, ed. Marin and Mandrillon, p.1460.
- [21] B. Chen, *The Longitudinal Collective Instabilities of Nonlinear Hamiltonian Systems in a Circular Accelerator*, Thesis, U. of Texas at Austin, May, 1995.
- [22] K.Y. Ng, *Potential-Well Distortion and Mode-Mixing Instability in Proton Machines*, Fermilab Report FN-630, 1995; K.Y. Ng, *Mode-Coupling Instability and Bunch Lengthening in Proton Machines*, Proc. 1995 Particle Accelerator Conference and International Conference on High-Energy Accelerators, Dallas, Texas, May 1-7, 1995, p.2977.
- [23] S.Y. Lee, K.Y. Ng, and D. Trbojevic, *Phys. Rev.* **E48**, 3040 (1993).